Dark matter theory

B.N.D. summer school

Gaétan Facchinetti

Service de Physique Théorique, C.P. 225, Université Libre de Bruxelles, Boulevard du Triomphe, B-1050 Brussels, Belgium

September 2024

These lecture notes aim at summarizing the basics of dark matter theory. After a brief introduction on the history of the dark matter discovery we focus on (particle) dark matter models and, in a second section, on the thermal production from chemical decoupling.

Contents

References

Books

- J. Bernstein (Cambridge University Press, 1988)
  Kinetic theory in the expanding universe
- E. W. Kolb, and M. S. Turner (Westview Press, 1994)
  The Early Universe
- H. Mo, F. van den Bosh, and S. White (Cambridge University Press, 2010)
  Galaxy Formation and Evolution
- S. Dodelson (Academic Press, 2003)
  Modern Cosmology

Reviews

- G. Bertone and D. Hooper (Rev. Mod. Phys. 90, 45002)
  A History of Dark Matter, arXiv:1605.04909
- P. J. E. Peebles (2017)
  How the Nonbaryonic Dark Matter Theory Grew, arXiv:1701.05837
- M. Cirelli, A. Strumia, and J. Zupan (2024)
  Dark Matter, arXiv:2406.01705

Lectures

- J. Ehlers (C.I.M.E. Summer Schools. Berlin, Heidelberg: Springer, 2011, pp. 301–388)
  General-relativistc kinetic theory of gases, Lecture notes
- D. Baumann (Lectures at the University of Cambridge)
  Cosmology Part III Mathematical Tripos, Lecture notes
- P. Salati (Lectures at ENS Lyon, 2017, in French)
  Introduction à l'astrophysique des particules, Lecture notes
- L. Lopez-Honorez (Lectures at ISAPP school 21)
  Dark Matter from Standard Model and Beyond, a selection of production mechanisms
  Lecture notes: part 1, part 2

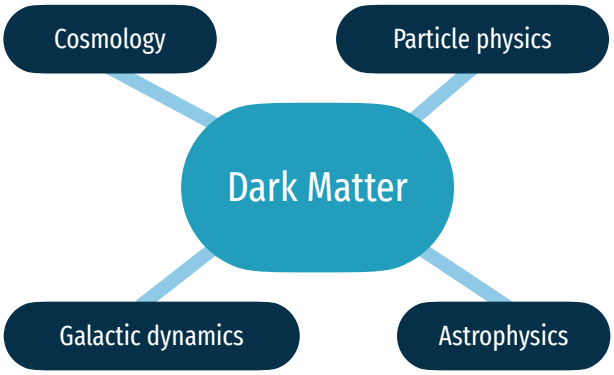

1 History and models

The study of dark matter involves different aspects of cosmology, astrophysics, galactic dynamics and particle physics. In this lecture we will mainly focus on the models and on particle physics although we will address the thermal production of the WIMP model that is tightly related to early Universe cosmology.

1.1 A brief history of the dark matter

In this chapter we address in very few details the history behind the discovery of dark matter. Here is a non exhaustive list of the many milestones that built our current knowledge of the (dark) Universe:

- 1846-1859: Explanation of the anomalous motion of Uranus by the presence of Neptune as predicted by Urbain Le Verrier.
- 1906: Henri Poincaré applied Lord Kelvin's theory of thermodynamics to celestial bodies, trying to assess the amount of *matière obscure* in the local Universe
- 1916: Albert Einstein explains the orbits of Mercury by introducing the general relativity, a more complete theory of gravity than that of Newton.
- 1922: Alexander Friedmann proposes an Universe in ongoing expansion.
- 1924: Edwin Hubble understands that many objects out there are not nebulae but galaxies and he measures their velocity.
- 1927: Georges Lemaitre independently finds the same results as Friedmann and uses Hubble's result to approximate the expansion rate
- 1929: With new observations Hubble refines the evaluation of the expansion rate
- 1932: Improving on Poincaré's idea, Jan Oort shows that the amount of dark / unseen bodies around should be $\rho_\odot \lesssim 0.05\ \mathrm{M}_\odot\,\mathrm{pc}^{-3}$ (in agreement with current observations, $\rho_\odot \sim 0.01 \pm 0.003\ \mathrm{M}_\odot\,\mathrm{pc}^{-3}$)
- 1933: Fritz Zwicky studies the Coma cluster. He founds that galaxies are faster than they should be considering the amount of luminous mass in the cluster, with the simple assumption that the cluster is a virialised object. More precisely he predicts a velocity dispersion of $\sim 80\ \mathrm{km\,s}^{-1}$ and measures $\sim 10^3\ \mathrm{km\,s}^{-1}$. At that time, many uncertainties (amongst which that on the value of the expansion rate of the Universe) and the possibe presence of non-luminous gas cast doubts on his conclusions advocating for the presence of *dunkle Materie* inside the cluster. Today, refined measurments show the conclusions were correct and that the non-luminous gas component should be subdominant.

- 1970: After preliminary works performed since the 1910's, Vera Rubin and Kent Ford refine the measurement of the rotation curve (circular velocity of stars or gas vs distance to the centre) for the Andromeda galaxy using the optical spectroscopy of ionized hydrogen (HII) emission regions. They find that it does not match the prediction obtained assuming that the mass of the galaxy exponentially decreases from its centre (as it is observed from the emitted light). More precisely, from Newtonian dynamics (general relativistic correction can safely be neglected here)

$$v_{\rm c}(R) \sim \sqrt{\frac{G_{\rm N} M(R)}{R}}\,, \tag{1}$$

  with $M(R)$ he mass enclosed inside the sphere of radius R. Thus, at large radii one should have $v_{\rm c} \propto R^{-1/2}$. In practice, they found $v_{\rm c} \sim$ cst., which, again, points towards the presence of unseen mass around the galaxy. An example of rotation curve is given for the M33 galaxy in the left panel of figure 2.

- 1970-1975: Discussions about the presence of unseen matter. Refined observations of the rotation curve using the 21cm line to probe the velocity of the neutral hydrogen (HI) gas shows the flatness of the rotation curve to larger radii. Moreover, similarities between the missing mass in galaxies and clusters are pointed out. These observations give a strong case in favour of dark matter existence.

- end of the 1980's: Little doubt is left thanks to the observation of flat rotation curve in other galaxies by Vera Rubin's and Albert Bosma's groups for instance.

- 2003-2020: With WMAP and now the Planck sattelite, the observations of the cosmic microwave background (CMB) anisotropies give new precise and quantitative information. Indeed, the observed distribution of the anisotropies can only be understood by considering that $\sim 84\%$ of the total matter content of the Universe is under the form of a non relativistic (also referred to as cold) collisionless fluid already present before recombination ($z \sim 1080$). The impact of the amount of dark matter in the Universe on the temperature anisotropies of the CMB has shown in the right panel of figure 2. As this quantity is extremely well measured by the Planck satellite, it sets strong constraints on the dark matter fraction. The main effect of the dark matter component is to maintain gravitational wells which are not destroyed by the radiation pressure, in which *baryonic* gas making up the stars (and referred to as *baryonic* since the mass is dominated by baryons) can accumulate as depicted in the illustration (a) of figure 1. In addition, the distribution of these potential wells is seen in the large scale surveys of galaxies (which formed preferentially were the baryonic gas accumulated) as a typical separation length. This effect is referred to as baryonic acoustic oscillations (BAO). Noteworthily, including the same amount of dark in the cosmological simulations, as that inferred from the cosmological observations, has allowed us to reproduce the structure of the Universe numerically.

1.2 Is there a dark matter? Why so cold?

All the evidences pointing towards the presence of a *dark matter* component making 84% of the Universe dicussed above manifests from gravitational interactions. Therefore, there are two possible explanations for *dark matter* nature. Either the relationship between mass and gravitational acceleration is not computed accurately within the framework of general relativity or some *invisible* mass is floating around galaxies and has been present at least before recombination. Hence, in the first scenario, *dark matter* does not exist per se and the solution would be to find the correct theory of gravity, completing general relativity. However, this is a tedious path, and although theories can be successful at explaining the local dynamics (e.g., MOdified Newtonian Dynamics – MOND [Milgrom, 1983]) their covariantization is challenging and explaining the CMB in these

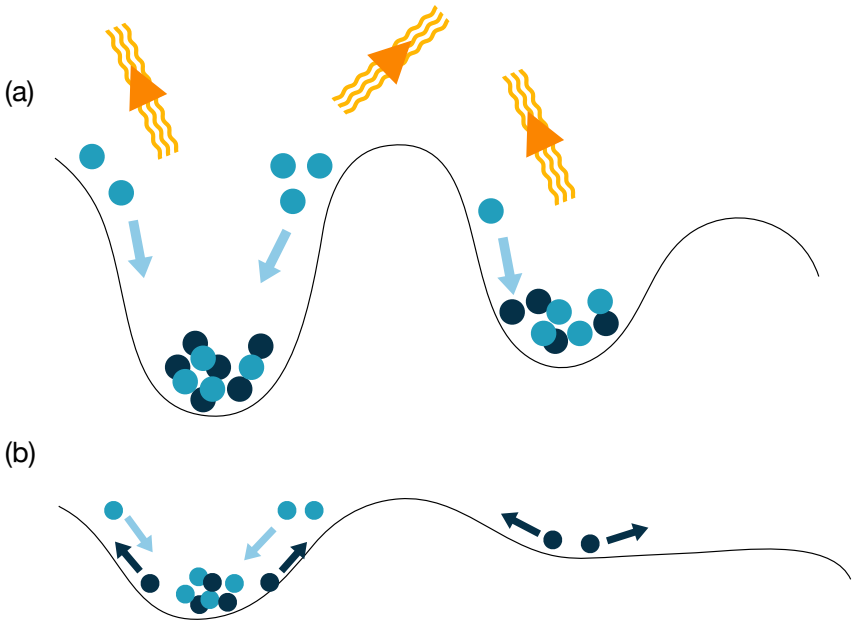

Figure 1: Illustrations representing (a) the baryons falling in the dark matter wells (b) the dark matter free-streaming smearing out the perturbations.

framework remains an open question [Famaey and McGaugh, 2012]. In the second scenario, one needs to consider all possible particle fields that are neutral (or quasi-neutral) under $U(1)_{\rm Q}$ of electromagnetism, massive and stable over the Universe lifetime. These lectures focus on the second solution.

> The two scenarios are often referred to as Mercurcy or Uranus-like solutions as they imply either a modification of the theory of gravity (as it was necessary to explain the perihelion precession of Mercury) or the presence of a new massive component (like Neptune to explain the anomalous orbit of Uranus).

Beside the observational hints discussed above, the ubiquitous presence of dark matter, able to efficiently respond to the gravitational perturbations seeded by inflation, further provides the most fundamental ingredient to our current theoretical understanding of structure formation. It also provides us with a clear understanding as for why galaxies and galaxy clusters are embedded into extended dark matter halos. In that picture, after recombination, dark matter, which dominates the energy budget of the Universe, drives the growth of the matter density fluctuations that survived the early epoch. After some time the over-dense regions become dense enough to collapse and virialise and they form bound objects called dark matter *halos*. All the structures seen have then been formed by the baryons falling in the middle of the halos, reaching a sufficient density to initiate star formation. In addition, note that the structure of the halos is fractal. Small halos are included into large halos themselves inside larger halos. Dwarf satellite galaxies of the Milky Way (e.g., Draco, Sculptor, ...) are bound to the surrounding Milky-Way halo, itself inside the halo containing the local group itself in the Virgo supercluster. The fractal structure of the halo can by analytically described by the excursion set theory, which predicts their mass distribution in a quantity referred to as the halo mass function.

One has to consider that the dark matter component is pressure-less and highly non-relativistic well before matter-radiation equivalence in order to understand the presence of clustering on the smallest scales observed. Indeed, dark matter particles with high velocity in the early Universe would have had time to free-stream out of the smallest over-dense region, smearing them out, before their growth. This is pictured in illustration (b) of figure 1. In other words, this effect induces a

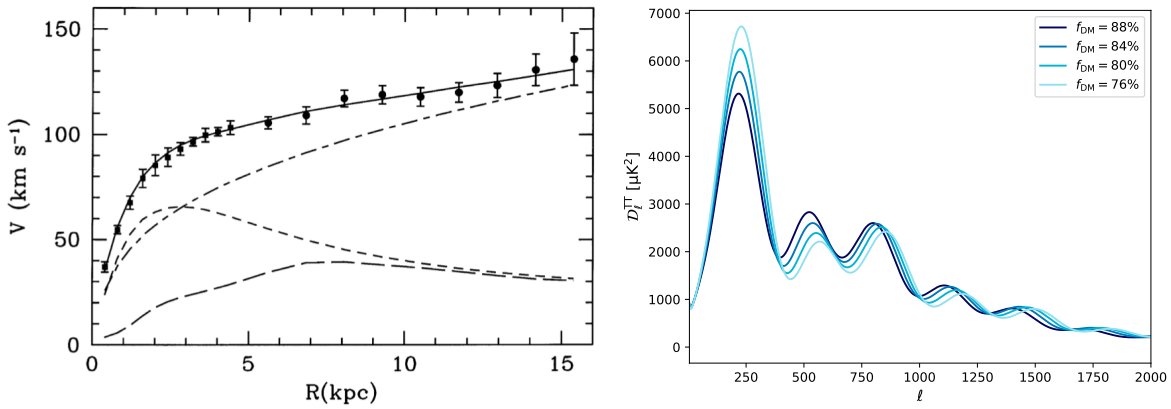

Figure 2: **Left panel**. Circular velocity with respect to the distance to the centre of the M33 galaxy. The points are the measured values with their error bars. The solid line is the total result from the model including DM. More precisely, the contribution of DM is shown in dash-dotted, the contribution of stars is shown in short dashes and the contribution of the gas in long dashes. Figure taken from [Corbelli and Salucci, 2000]. **Right panel**. Temperature anisotropy power spectrum of the CMB for various dark matter fractions (for a fixed total matter abundance and the other parameters set to the best fit value of [Aghanim et al., 2020]). The darker the curve the more dark matter. Figure obtained running `CLASS` [Blas et al., 2011].

cut-off on the power spectrum (the two-point correlation function of the matter density) at small scales. The current constraints allow for models that are then called warm or cold dark matter (WDM or CDM). For the past decade, the dark matter community as been puzzled by a series of small-scale issues, that are discrepancies between observations and prediction (from simulations). Amongst those issues were the missing satellite problem and the too-big-to-fail problem. The first one was the fact that the Milky-Way halo was hosting less dwarf galaxies than expected. The second is that there should be large enough halos in the Milky-Way that could not have failed forming small galaxies but that we do not see. These were claimed as strong indication for WDM that reduces the number of small halos and thus of dwarf galaxies. However, due to the discovery of more dwarf galaxies and a better treatment of the baryonic physics in the cosmological simulations (that were previously run without) the discrepancies have vanished. The cold dark matter scenario, corresponding to the smallest velocity dispersion, thus remains the standard scenario.

Nonetheless, it is worth noting that other small-scale issues are still open questions. The reason why some galaxies have a cored (flat) dark matter distribution in their centre remains uncertain and is called the *core-cusp* issue. More puzzling is the *diversity* issue, the fact that similar galaxies (with outskirts stars of comparable velocity) can either have a spiky distribution of dark matter in their centre or a cored one. In the other hand one also observes a tight correlation between the acceleration due to baryons and the total observed acceleration in galaxies. The smallness of the scatter makes the diversity issue even more challenging as for a given distribution of baryons one should not expect significantly different dark matter distributions. A dark matter that can self interact, could alleviate some of these tension by dynamically forming a core. However, this scenario is constrained for example by the bullet-cluster, showing two halos colliding whose mass distribution can be reconstructed with gravitational lensing techniques. As this observation shows no self-interaction, it places an upper bound on the corresponding cross-section. See Ref. [Bullock and Boylan-Kolchin, 2017] for a review.

The next step now is to first look into the standard model of particle physics whether one can find a particle with all the good properties to be the dark matter.

		$SU(3)_{\rm C}$	$SU(2)_{\rm L}$	Y	T^3	Q
$L_{\rm L}$	$\nu_{\ell,{\rm L}}$	**1**	**2**	-1	1/2	0
	$\ell_{\rm L}$				-1/2	-1
$\ell_{\rm R}$		**1**	**1**	-2	0	-1
Q_L	u_L	**3**	**2**	1/3	1/2	2/3
	d_L				-1/2	-1/3
$u_{\rm R}$		**3**	**1**	4/3	0	2/3
$d_{\rm R}$		**3**	**1**	-2/3	0	-1/3
H	H^+	**1**	**2**	1	1/2	+1
	H^0				$-1/2$	0

Table 1: A selection of the standard model content with associated charges

1.3 A quick look into the standard model

The standard model is a non-abelian quantum field theory based on a partially and spontaneously broken gauge symmetry

$$G = SU(3)_{\rm C} \otimes SU(2)_{\rm L} \otimes U(1)_Y \, .$$

The $SU(2)_{\rm L} \otimes U(1)_Y$ part corresponds to the electroweak sector that unifies the electromagnetic and weak interactions. The L subscript stands for *left* as the $SU(2)$ group only acts on left-handed particles. Interactions are mediated via particles in the adjoint representation of the group: the gluons g for the strong interaction and the massless bosons W^1, W^2, W^3 and B for the electroweak interaction. At low energy ($E < \Lambda_{\rm EW} \sim 250$ GeV) the Brout-Englert-Higgs field H, coupled in a gauge-invariant way to fermions, falls at the bottom of a potential well, gets a vacuum expectation value (VEV) usually denoted $v \equiv \langle H \rangle$, and induces the spontaneous symmetry breaking, $SU(2)_{\rm L} \otimes U(1)_Y \to U(1)_Q$. The group $U(1)_Q$ describes the electromagnetic interactions with Q the standard electromagnetic charge. Denoting $\hat{\sigma}^3$ the third Pauli matrix, then $\hat{T}^3 \equiv \hat{\sigma}^3/2$ is the third generator of $SU(2)_{\rm L}$ and we define the electromagnetic charge operator as $\hat{Q} \equiv \hat{T}^3 + Y/2$ with Y the hypercharge. The subsequent Goldstone bosons can be 'gauged-out', which transforms the W and B fields into three massive fields (with longitudinal polarisation) W^+, W^-, Z^0. The remaining massless field corresponds to the photon.

The spin-1/2 content of the standard model (with the associated charges) is summarised in table 1.3. There is only one entry with $Q = 0$ which corresponds to the neutrinos. Although they have no mass term in the standard model, they have to be massive since we observe flavour oscillations. Even if the origin of the mass is yet to be determined, that makes the neutrinos massive, uncharged particles that can very well make the dark matter.

Denoting m_i the masses of the three neutrinos, one can evaluate their total abundance in the Universe today as being [Lesgourgues and Pastor, 2006]:

$$\Omega_{\nu,0} h^2 \equiv \frac{\rho_{\nu,0}}{\rho_{\rm c}} h^2 = \sum_{i=1}^{3} \frac{m_i}{93.14 \text{ eV}} \tag{2}$$

where $\rho_c \equiv 3H_0^2/(8\pi G_{\rm N}) \sim 1.27 \times 10^{11}$ $\mathrm{M_\odot\,Mpc^{-3}}$ is the critical density of the Universe today, $h \sim 0.67$ is the Hubble parameter and $\rho_{\nu,0}$ is the energy density of neutrinos today. While the best constraints from ground experiments are of the order $m_i < 0.8$ eV - with a 90% confidence level [Aker et al., 2022] – that roughly gives $\Omega_{\nu,0} h^2 < 2.6 \times 10^{-2}$. The CMB puts a bound $\sum_i m_i < 0.24$ eV (with a 95% confidence level from Planck [Aghanim et al., 2020]) that yields $\Omega_{\nu,0} h^2 < 2.6 \times 10^{-3}$, far below the inferred value for the total dark matter $\Omega_{\rm c,0} h^2 = 0.12$. In addition, if the dark

matter was exclusively made of neutrinos it would be classified as hot dark matter because ultra relativistic at matter-radiation equality, due to their small mass. This is however not supported by observations (e.g. from Lyman-α) which strongly favour hierarchical structure formation. Therefore it would be difficult to explain the presence of galaxies. Besides, the mass of fermionic dark matter particles is also constrained by their phase-space distribution in galaxies to $m \geq 1.7$ keV with the Tremaine-Gunn bound [Tremaine and Gunn, 1979, Boyarsky et al., 2009].

Because if not for the neutrinos no other elementary particle fit the requirements for being dark matter in the standard model, it is necessary to look for beyond standard solution.

1.4 If not in the standard model, what else?

As discussed above, one needs to rely on extensions of the standard model to incorporate dark matter. It actually turns out that, while the standard model allows for predictions of subatomic properties or processes which have been tested to unprecedented precision, it is not devoid of issues. For instance, it does not allow to fully understand the hierarchy of particle masses, the hierarchy between the Planck and electroweak scales, the specificity of neutrinos (initially described as massless and only left-handed particles), and it does not incorporate gravity even when it gets relevant in the very high-energy limit. Other issues are of observational nature: it does not provide an explanation to the asymmetry between matter and antimatter, nor to inflation. Therefore, interesting theoretical solutions are given by extensions/modifications of the standard model that can solve at least one problem inherent to particle physics and can at the same time provide a good dark matter candidate.

1.4.1 Sterile neutrinos

Let us focus back on the neutrinos. As seen above, although in the standard model there is no mass terms for the neutrinos, they must be massive to produce flavour oscillations. Assuming that no right handed neutrino exists, the only solution would be for neutrinos to be Majorana particles. Let us define the 4-component spinor for a single neutrino flavour (generalisation is straightforward)

$$\psi_{\nu,\mathrm{L}} = \begin{pmatrix} \nu_\mathrm{L} \\ 0 \end{pmatrix} \quad \text{and} \quad \psi^c_{\nu,\mathrm{L}} = \gamma^0 C \psi^*_{\nu,\mathrm{L}} = \begin{pmatrix} 0 \\ i\sigma^2 \nu^*_\mathrm{L} \end{pmatrix} \tag{3}$$

with C the charge conjugation matrix satisfying $C = i\gamma^2\gamma^0$ in the chiral basis. One must be careful as, despite the L notation in its name, it is clear from the equation above that $\psi^c_{\nu,\mathrm{L}}$ is a left right handed spinor. A neutrino Majorana spinor can then be defined as $\nu_\mathrm{M} = \psi_{\nu,\mathrm{L}} + \psi^c_{\nu,\mathrm{L}}$ as it automatically satisfy the Majorana condition $\nu^c_\mathrm{M} = \nu_\mathrm{M}$. Then a simple mass term would be

$$\mathcal{L}_\mathrm{Majorana} = -\frac{1}{2} m_\mathrm{M} \overline{\nu_\mathrm{M}} \nu_\mathrm{M} = -\frac{1}{2} m_\mathrm{M} \left(\overline{\psi^c_{\nu,\mathrm{L}}} \psi_{\nu,\mathrm{L}} + \overline{\psi_{\nu,\mathrm{L}}} \psi^c_{\nu,\mathrm{L}} \right) = -\frac{1}{2} m_\mathrm{M} \nu^\dagger_L i\sigma^2 \nu^*_L + \mathrm{h.c.} \tag{4}$$

However, under a gauged transformation of $U(1)_Y$ one can check that by properties of ν_L then $\psi_\nu \to e^{i\alpha(x)Y/2}\psi_\nu$ (hypercharge 1) while $\psi^c_\nu \to e^{-i\alpha(x)Y/2}\psi_\nu$ (hypercharge -1). Therefore, the mass terms is not invariant under $U(1)_Y$ of the standard model. Because the electric charge is 0, it implies that it breaks the isospin charge T^3 by 1. There is no way to fix that within the standard model.

A solution to the problem is thus to introduce a right handed neutrino ν_R (or $\psi_{\nu,\mathrm{R}}$ in 4-components notation). Then, we can straightforwardly add a term $y\overline{L}\tilde{H}\nu_R$ with its hermitian conjugate, where $\tilde{H} = i\sigma^2 H^*$, $L = (\psi_{\nu,\mathrm{L}}, \psi_{e,\mathrm{L}})^T$ and H the Brout-Englert-Higgs doublet. After spontaneous symmetry breaking $< \tilde{H} >= (v/\sqrt{2}\ 0)^T$ and it yields a Dirac mass term for the neutrinos

$$\mathcal{L}_\mathrm{Dirac} = -y\frac{v}{\sqrt{2}} \overline{\psi_{\nu,\mathrm{L}}} \psi_{\nu,\mathrm{R}} + \mathrm{h.c.} \tag{5}$$

such that we can define the Dirac mass as $m_\mathrm{D} = yv/\sqrt{2}$.

> You can check that the new term is invariant under $U \in SU(2)_{\rm L}$ because $\overline{L} \to \overline{L}U^\dagger$ and $\tilde{H} \to i\sigma^2 U^* H^* = iU\sigma^2 H^* = U\tilde{H}$, where the last equality comes from the fact that $\sigma^2 U^* = U^* \sigma^2$.

Interestingly, because $\tilde{H}$ and L both have hypercharge -1 and transform as a doublet of $SU(2)_{\rm L}$, the new right handed neutrino, must be a singlet of both $SU(2)_{\rm L}$ and $U(1)_Y$. For this reason it is referred to as a *sterile* neutrino, while the standard model neutrinos are called active. There are no restrictions then for $\psi_{\nu,{\rm R}}$ to have a Majorana mass term if we assumt that it is a Majorana particle. Then, the most general mass term allowed in the Lagrangian becomes

$$\mathcal{L}_{\rm Mass} = -\frac{1}{2}\begin{pmatrix}\overline{\psi_{\nu,{\rm L}}} & \overline{\psi^c_{\nu,{\rm R}}}\end{pmatrix}\begin{pmatrix}0 & m_{\rm D}\\ m_{\rm D} & m_{\rm M,R}\end{pmatrix}\begin{pmatrix}\psi^c_{\nu,{\rm L}}\\ \psi_{\nu,{\rm R}}\end{pmatrix} + {\rm h.c.} \tag{6}$$

The product of the eigenvalues m_1, m_2 of the mass matrix is $m_{\rm D}^2$ (in absolute value). Therefore, in order for the physical left handed neutrinos to have a small mass (as observed), the sterile neutrino must have a conversely large mass. This is the basics of the seesaw mechanism to attribute a mass to the neutrinos. For our concern, we have introduced here a new massive field, singlet of the standard model. Therefore, the sterile neutrino could be a good dark matter candidate [Dodelson and Widrow, 1994, Shi and Fuller, 1999]. Nonetheless, the physical sterile neutrino $N_{\rm R}$ is a mixed state of the interaction sterile neutrino and the interaction left handed neutrino. Let us call $\psi_{i,{\rm L}}$ the two mass eigenstates,

$$\begin{pmatrix}\psi_{1,{\rm L}}\\ \psi_{2,{\rm L}}\end{pmatrix} = P^T\begin{pmatrix}\psi_{\nu,{\rm L}}\\ \psi^c_{\nu,{\rm R}}\end{pmatrix} \tag{7}$$

with P the orthogonal matrix

$$P = \begin{pmatrix}\cos\theta & \sin\theta\\ -\sin\theta & \cos\theta\end{pmatrix} \quad \text{such that} \quad P^T\begin{pmatrix}0 & m_{\rm D}\\ m_{\rm D} & m_{\rm M,R}\end{pmatrix}P = \begin{pmatrix}m_1 & 0\\ 0 & m_2\end{pmatrix} \tag{8}$$

and where θ is the mixing angle. We can thus define two Majorana neutrinos

$$\nu_{\rm M,i} = \psi_{i,{\rm L}} + \psi^c_{i,{\rm L}} \tag{9}$$

and for $\theta \sim 0$ we can associate the sterile neutrino with $\nu_{\rm M,2}$. Because of the mixing with the active neutrino though, the sterile neutrino can slowly decay into a left handed neutrino and a photon according to the triangle diagram with a W boson exchange. As seen in figure 3, constraints on the mixing angle are set from X-ray searches and from the *warmness* of the produces sterile neutrino assuming they make all of the dark matter content. Indeed, $\sim$ keV dark matter, produced with a too large velocity can smear out structure formation on observable scales.

1.4.2 The IMPs: the WIMP, the FIMP and the SIMP

Weakly interacting massive particles (WIMPs) encompassed a broad class of dark matter model that have received a lot of attention during the last decades. They are neutral, cold and stable particles with a mass in the GeV-TeV range, interacting at the weak-scale with standard model particles. There are two reasons for the popularity of the WIMPs. Firsty, their thermal production mechanism (which we will detail in the next section) in which they are in thermal equilibrium with the primordial plasma before decoupling, naturally gives the correct dark matter abundance without fine tuning [Lee and Weinberg, 1977, Binetruy et al., 1984]. Secondly, they easily arise in supersymmetric models [Gervais and Sakita, 1971, Neveu and Schwarz, 1971, Ramond, 1971, Wess and Zumino, 1974] and in models with extra dimensions [Kaluza, 1921, Klein, 1926]. In supersymmetry, for instance, a combination of the W, B and two Brout-Englert-Higgs bosons superpartners called wino, bino and higgsinos make the four neutralino mass eigenstates. Assuming R-parity to avoid proton decay, the

lightest of the neutralinos (also called LSP for lightest supersymmetric particle) is the prototypical example of a WIMP. Today the pressure put on the parameter space by the LHC, and by direct and indirect detection experiments has slightly reduced the interest of the community, even though the WIMP still remains a plausible simple and minimal candidate [Leane et al., 2018].

Considering smaller couplings to the standard model leads to the feebly interacting massive particles (FIMPs) scenario, with a slightly different thermal production mechanism where thermal equilibrium with the primordial plasma is never reached. More generally, a plethora of similar models that distinguish themselves by a different production mechanism have been considered as the WIMPZILLA (with a mass up to 10^{16} GeV), the exponential growth dark matter produced from $\chi + \psi \to \chi + \chi$ processes (where χ is the dark matter and ψ a standard model particle) or the strongly interacting massive particle (SIMPs) produced from $3 \to 2$ processes. The list is, however, too long to be exhaustive on these lecture notes.

1.4.3 Axion(-like) particles

In full generality, one needs to introduce a CP-violating term in the SM Lagrangian

$$\mathcal{L}_\theta = -\frac{\overline{\theta}}{32\pi^2}\mathrm{Tr}\left[\tilde{G}_{\mu\nu}G^{\mu\nu}\right] \tag{10}$$

where $G^{\mu\nu}$ is the gluon field strength tensor and $\tilde{G}^{\mu\nu} = \epsilon^{\mu\nu\rho\sigma}G_{\rho\sigma}/2$. In this term, the coupling constant is related to non trivial topological properties of $SU(3)_\mathrm{c}$ and to the associated instantons. Indeed, would not it be for the instantons, as this term can be rewritten as a current derivative, it would not produce any physical effect at all (as it is the case in QED). However, due to the instantons, it contributes non-perturbative effects. In addition, this term can not be removed by chiral rotations but it is shifted to $\theta = \overline{\theta} + \arg(\det\mathcal{M}_u\mathcal{M}_d)$ where $\mathcal{M}_u$ and $\mathcal{M}_d$ are the quark mass matrices. So far so good but, it also contributes to the electric dipolar moment of the neutron $d_\mathrm{n} \simeq 3.6 \times 10^{-16}\theta e$ which is experimentally constrained. Current observations show that $\theta \leq 10^{-10}$, which can then be considered a problem, called the strong-CP problem, if one is sceptical about such a large degree of fine tuning.

A possible solution is to introduce a new field, called the axion, coupled to $\tilde{G}G$ with a dynamics that naturally leads to the cancellation of θ. Several models for the axion have been introduced: the Peccei-Quinn-Weindberg-Wilczek (PQWW) axion [Peccei and Quinn, 1977, Weinberg, 1978, Wilczek, 1978], the Kim-Shifman-Vainshtein-Zacharov (KSVZ) axion [Kim, 1979, Shifman et al., 1980], and the Dine-Fishler-Srednicki-Zhitnitsky (DFSZ) axion [Dine et al., 1981, Zhitnitskij, 1980]. The first one, however, is already ruled out, for instance, by beam dump experiments. The axion ϕ is introduced as the pseudo Nambu-Golstone boson associated to a new $U(1)_\mathrm{PQ}$ chiral symmetry that is spontaneously broken at an energy scale $f_a \gg \Lambda_\mathrm{QCD} \sim 150$ MeV. When the primordial plasma cools down below Λ_QCD, the axion gets a periodic potential, rolls down to a minimum and oscillates, forming a zero-momentum condensate with the minimum such that $\theta + \phi = 0$. As the introduction of the axion produces the same coupling than in Eq. (10), replacing $\overline{\theta}$ with ϕ, this gives a natural explanation for the smallness of the electric dipolar moment of the neutron. The formation process of the axions, unlike that of the WIMP, is called non-thermal and their mass is then roughly given by

$$m_a \sim 10\,\mu\mathrm{eV}\left(\frac{10^{12}\ \mathrm{GeV}}{f_a}\right). \tag{11}$$

Thus, even if light, axions are massive and *cold* particles, thus good DM candidates. Depending on when the Peccei-Quinn symmetry is broken and on the initial value of the axion field, the correct abundance of DM can be achieved for 10^9 GeV $\lesssim f_a \lesssim 10^{15}$ GeV, which corresponds to a mass range 10^{-9} eV $\lesssim m_a \lesssim 10^{-3}$ eV. This is of course a very rough window but gives an idea of the scales. See Ref. [Marsh, 2016] for a review.

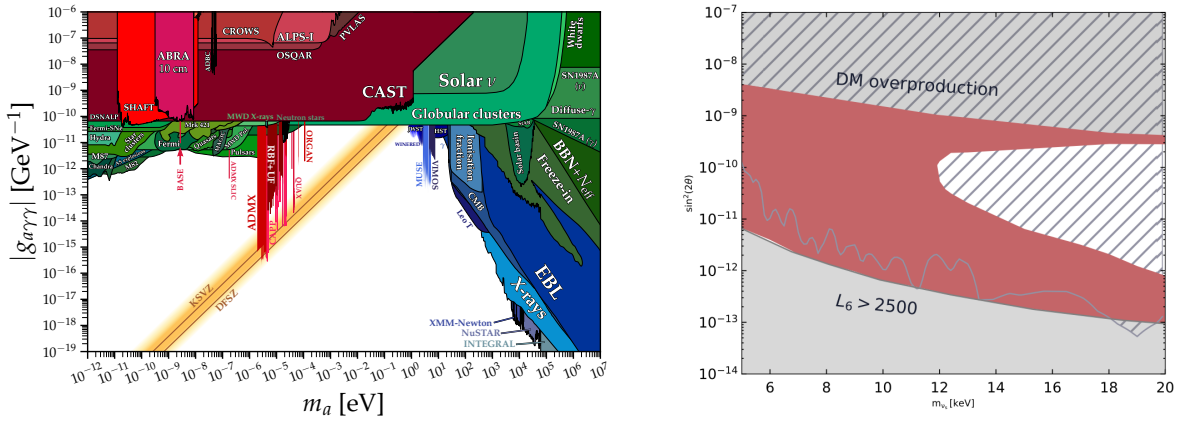

Figure 3: Current limits on the axion-photon coupling (left panel, figure taken from Ref. [O'Hare, 2020]) and sterile neutrino mixing angle (right panel, figure adapted from Ref. [Dekker et al., 2022]). The hashed gray lines on the right panel are the current X-ray constraints, the bottom grey region is the a constraint on the lepton asymmetry bounded by the Big-Bang nucleosynthesis. The red contour is excluded due to the warmness of the sterile neutrinos produced with the Shi-Fuller mechanism from the number counting of dwarf galaxies in the Milky-Way.

> The Peccei-Quinn symmetry is said to be chiral as it acts on a field ψ as $\psi \to e^{iq_{\rm PQ}\phi/f_a\gamma^5}\psi$ with $q_{\rm PQ}$ the Peccei-Quinn charge.

Even if the QCD axion does not exist or does not make all of the dark matter, it has paved the way to more generic studies of axion-like particles or ultra-like axions that generalise the QCD axion but are not necessarily related to the strong CP problem. The latter, make what is called fuzzy dark matter as their mass (down to $m_a \sim 10^{-22}$ eV) corresponds to a wavelength up to $\lambda \sim 0.4$ pc (astrophysical scale).

An interesting property of the axion(-like) field is its coupling to the photon field and to the standard model fermions according to the Lagrangian

$$\mathcal{L}_{\phi,\,\rm SM} = \frac{1}{4} g_{a\gamma\gamma}\phi F_{\mu\nu}\tilde{F}^{\mu\nu} - \phi\sum_{\psi} g_{\psi}^{\rm p}(i\overline{\psi}\gamma^5\psi) - \phi\sum_{\psi} g_{\psi}^{\rm s}\overline{\psi}\psi \tag{12}$$

where ψ are standard model fermions. The first term on the left should vanish as it can be rewritten as a total derivative, but is actually an effective dimension 5 interaction term arising at loop level from the triangle diagram with one axion in, two photons out and a fermion charged under $U(1)_{\rm PQ}$ running in the loop. In figure 3 we show the current constraints on the axion-photon coupling. Even though the highest values of $g_{a\gamma\gamma}$ have been ruled out, the parameter space remains largely open at small masses. Haloscopes (cavities in which we try to transform surrounding axions into photons thanks to a strong magnetic field) are amongst the most promising tools. In addition, the coupling to electrons has recently attracted a lot of attention due to the claimed electron recoil excess in XENON-1T experiment [Aprile et al., 2020], which could have been explained using axions. Unfortunately, the excess has vanished after a longer observational campaign and new analyses [Aprile et al., 2022].

1.4.4 The vector portal: dark photons and millicharged dark matter

In this model, we assume a new symmetry $U(1)'$ group. This new gauge group implies this existence of a massive or massless dark photon, that is allowed to mix (at least at the loop level if some fields are charged under both $U(1)'$ and $U(1)_Y$) with the standard photon with a mixing term of the form

$$\mathcal{L}_{\rm mix} = -\epsilon F'_{\mu\nu}B^{\mu\nu} \tag{13}$$

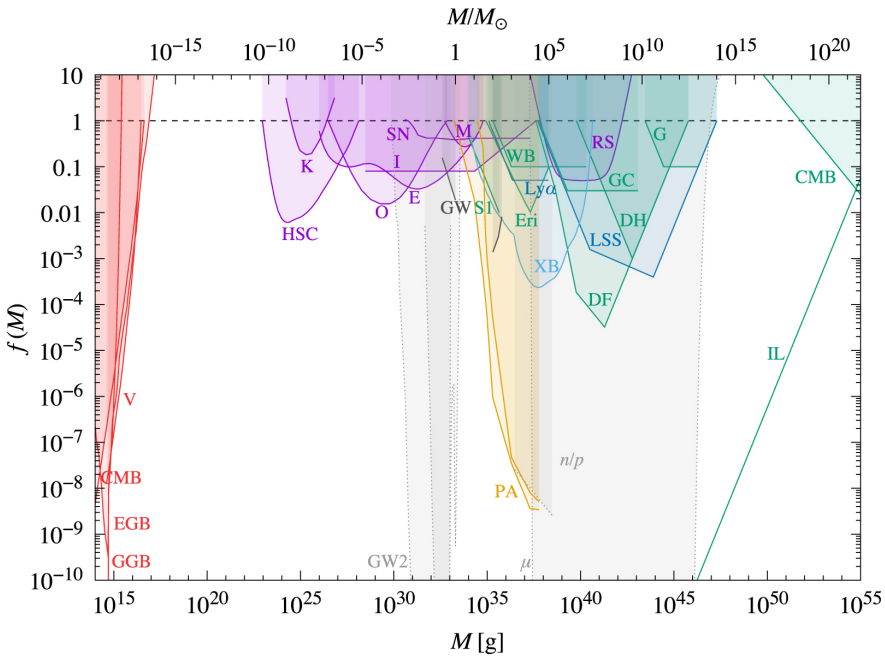

Figure 4: Compilation of constraints on the fraction of dark matter that can be in the form of PBHs. Figure taken from Ref. [Carr et al., 2021]

with F' the $U(1)'$ field strength tensor and $B^{\mu\nu}$ the $U(1)$ field strength tensor. A massive dark photon, if light enough to not decay to fast into standard model particles can be the dark matter. We can also add a matter field χ, charged under $U(1)'$ with the Lagrangian

$$\mathcal{L}_{\rm DS} = -\frac{1}{4}F'_{\mu\nu}F'^{\mu\nu} + \frac{1}{2}m'^2_A A'_\mu A'^\mu + i\overline{\chi}\not{D}'\chi - m_\chi\overline{\chi}\chi\,, \tag{14}$$

where $D'_\mu = \partial_\mu - g_D A'_m u$ with A'_μ the dark photon and g_D the associated dark charge. If the dark photon is twice more massive than the field χ then the $A' \to \chi\chi$ decay is allowed. Then, if $g_{\rm D}$ is large enough χ becomes the dark matter candidate. Finally, if the dark photon mass goes to 0, then the mixing with the classical photons, gives an small effective electromagnetic charge to χ, hence the name of millicharged dark matter.

In addition, if the dark photon directly couples to the standard model particles, it is referred to as a Z'. This would be the case when gauging the non anomalous accidental symmetries of the standard model setting, for instance, $U(1)' = U(1)_{B-L}$ under which quarks have a charge $+1/3$ and lepton a charge -1.

1.4.5 Primordial black holes

Primordial black holes [Zel'Dovich and Novikov, 1966, Hawking, 1971, Carr and Hawking, 1974] (PBH) are a good DM candidate. PBHs could form, for instance, in the primordial universe from rare and extremely high density fluctuations that collapse directly to BHs right after entering the horizon, after inflation. Since collapsing from gravitational instabilities, their formation are boosted each time the radiation pressure in the universe drops. This happens for instance at the QCD phase transition [Jedamzik, 1997], or any other transition when relativistic degrees of freedom disappear (e^+e^- annihilation, etc.) – see the next section. The abundance of PBHs depends on the amplitude of the primordial power spectrum, and should be extremely small if the latter were at the level constrained by Planck. However, the amplitude is not constrained on small scales, and could actually be such that PBHs represent a significant fraction, if not all, of the dark matter in the universe. Present at the time of last-scattering and if numerous enough they provide the non-baryonic mass

necessary to understand the anisotropies of the CMB, playing the role of dark matter. This scenario faces observational pressure too, with the microlensing studies constraining MACHOs, with BBN and CMB, with γ-ray and cosmic- ray instruments - due to Hawking's radiation - and with many other probes. A compilation of the current constraints on the fraction of dark matter into the form of PBH is given in figure 4. One window remains open for PBHs with mass 10^{17} g $< m_{\rm PBH} < 10^{22}$ g. Finally, let us point out that PBHs have also regained interest thanks to the latest observations of black holes binary mergers with the gravitational waves detectors LIGO/Virgo [Abbott et al., 2019]. In the scenario inspired by LIGO/Virgo the fraction of DM in the form of PBHs could be established at $\sim 10^{-3}$ even if a total fraction of 1 is still possible in some models.

2 Thermal production of dark matter

In this second section we address the question of the thermal productions of particles in the Universe. Although this scenario does not apply to axions for instance, it remains a widely studied mechanism of production. In particular we will focus on the *vanilla* WIMP *freeze-out* and the so-called WIMP-miracle. To that end, we first review the Boltzmann equation in a non-euclidean space-time manifold and apply it to the FLRW expanding Universe. Then we detail the thermal evolution of the Universe in its first second and, finally, discuss the creation of dark matter.

2.1 Boltzmann's equation

The ensemble average number of occupied states in a volume of phase space (positions and on-shell momenta) can be written according to a single function f called the one-point phase-space distribution function (PSDF). In curve space time of metric g, the number density current and stres-energy density tensor of a given species are defined as the first and second moments of the phase space distribution function as

$$\begin{aligned} n^\mu &\equiv \frac{g_f}{(2\pi)^3}\int f(x^\mu, p^i) p^\mu \frac{\sqrt{-g}}{\hat{p}_0}\frac{\epsilon_{abc}}{3!}\mathrm{d}p^a \wedge \mathrm{d}p^b \wedge \mathrm{d}p^c \\ T^{\mu\nu} &\equiv \frac{g_f}{(2\pi)^3}\int f(x^\mu, p^i) p^\mu p^\nu \frac{\sqrt{-g}}{\hat{p}_0}\frac{\epsilon_{abc}}{3!}\mathrm{d}p^a \wedge \mathrm{d}p^b \wedge \mathrm{d}p^c \end{aligned} \tag{15}$$

where g_f is the number of degrees of freedom and ϵ_{abc} the tensor of Levi-Cevita. Moreover, $\hat{p}_0 = \hat{p}_0(x^\mu, p^i)$ is the on-shell energy satisfying $g_{\mu\nu}p^\mu p^\nu = m^2$. One can show (see Ehlers for a complete proof) that the PSDF follows Boltzmann's equation:

$$L[f] = C[f], \tag{16}$$

where C is the collision operator and L is the Liouville's vector describing the geodesic flow in phase space. The latter takes the form

$$L \equiv p^\mu \frac{\partial}{\partial x^\mu} - \Gamma^i_{\mu\nu} p^\mu p^\nu \frac{\partial}{\partial p^i} \tag{17}$$

where $\Gamma^i_{\mu\nu}$ are the Christoffel's symbols. For a collisionless species (i.e., that does not interact), $C = 0$ and Boltzmann's equation reduced to Liouville's equation. Boltzmann's equation encodes how the geometry of the Universe on one side and the interactions between species on the other side both impact their distributions.

> In full generality the collision term should depend on the n-point PSDF between each interacting species. However, assuming *molecular chaos*, that is, the momenta of colliding particles are uncorrelated and do not depend on their position, the two-point PSDF can be written as the product of two one-point PSDFs.

Assuming a flat FLRW Universe with scale factor $a(t)$,

$$\mathrm{d}s^2 = \mathrm{d}t^2 - a^2(t)(\mathrm{d}x^2 + \mathrm{d}y^2 + \mathrm{d}z^2)\,, \tag{18}$$

due to the homogeneity and isotropy the phase space distribution function does only depend on t and $p \equiv (-g_{ij}p^i p^j)^{1/2} = a(\delta_{ij}p^i p^j)^{1/2}$ the 3-momentum norm. The action of the Liouville's operator on the PSDF f can then be written

$$L[f](t,p) = E(p)\left(\frac{\partial f}{\partial t} - H(t)p\frac{\partial f}{\partial p}\right) \tag{19}$$

with $E(p) = (m^2 + p^2)^{1/2}$ the particle energy and H the Hubble rate. The term proportional to H arises from the influence of the expansion of the Universe. Morever, from Eq. (15) the number density, energy density and pressure take the form

$$\begin{aligned} n(t) &\equiv n^0 = \frac{g_f}{2\pi^2}\int f(t,p)p^2\mathrm{d}p \\ \rho(t) &\equiv T^{00} = \frac{g_f}{2\pi^2}\int f(t,p)E(p)p^2\mathrm{d}p \\ p(t) &\equiv \frac{1}{3}\mathrm{Tr}\left\{T^{ij}\right\} = \frac{g_f}{6\pi^2}\int f(t,p)\frac{p^4}{E(p)}\mathrm{d}p \end{aligned} \tag{20}$$

> Exercise 1: Boltzmann's equation in FLRW
>
> Show that, integrating over Liouville's vector applied on the PSDF,
>
> $$\frac{\mathrm{d}n}{\mathrm{d}t} + 3Hn = \frac{g_f}{2\pi^2}\int C[f]\frac{p^2}{E(p)}\mathrm{d}p\,. \tag{21}$$
>
> Conclude that, for a collisionless species, $n \propto a^{-3}$.

Although this introduction of the Boltzmann equation was brief, we already have everything we need for the rest of the discussion with Eqs. (20, 21). Let us now describe the thermal evolution of the Universe.

2.2 Thermal history of the Universe

Dark matter creation in thermal scenarios, which we focus on, is tightly related to the thermodynamics of the primordial bath filling the Universe. In this section let us derive the main equations describing the evolution of standard model species with the Universe expansion. The thermodynamical equilibrium distribution of interacting species in a bath is defined as the PSDF which conserves the flow of entropy

$$S^\mu \equiv -\frac{1}{2\pi^2}\sum_i g_{f,i}\int \left[f_i \ln f_i - \eta_i(1+\eta_i f_i)\ln(1+\eta_i f_i)\right]\frac{p^\mu p^2}{E(p)}\mathrm{d}p\,, \tag{22}$$

where the sum runs over all interacting species in the bath and $\eta_i = -1$ (resp. $+1$) for fermions (resp. bosons). Rewriting S^μ in terms of an integral over the collision operator and inspecting the terms in that intergal we arrive at the H-theorem, which states that

$$\nabla_\mu S^\mu \geq 0\,, \tag{23}$$

and that the minimum is reached for (in the rest frame of the fluid)

$$f_{\mathrm{eq},i}(t,p) = \frac{1}{e^{\beta E(p) - \alpha_i} - \eta_i} \quad \forall \text{ species } i \tag{24}$$

with α_i and $\beta > 0$ constants to determine. To that end we introduce the entropy density as total entropy per unit of volume (in the rest frame of the fluid) $s = S^0$. We derive below thermodynamical relations to identify α_i and β with thermodynamical quantities. This is the goal of the following exercises below.

Exercise 2: entropy density

Show that for a fluid in equilibrium

$$s_{\rm eq} = -\sum_i \alpha_i n_{{\rm eq},i} + \beta \left[\rho_{\rm eq} - \sum_i \eta_i \frac{g_{f,i}}{2\pi^2} \int_m^\infty \ln\left(1 - \eta_i e^{-\beta[E-\alpha_i]}\right) E\sqrt{E^2-m^2}\,{\rm d}E \right] \tag{25}$$

and that, after a change of variable in the integral,

$$s_{\rm eq} = -\sum_i \alpha_i n_{{\rm eq},i} + \beta \left[\rho_{\rm eq} + P_{\rm eq}\right] . \tag{26}$$

with $\rho_{\rm eq} = \sum_i \rho_{{\rm eq},i}$ and $P_{\rm eq} = \sum_i P_{{\rm eq},i}$.

Exercise 3: laws of thermodynamics

The pressure at equilibrium is a function of α_i and β therefore we can write

$${\rm d}P_{\rm eq} = \sum_i \frac{\partial P_{\rm eq}}{\partial \alpha_i}{\rm d}\alpha_i + \frac{\partial P_{\rm eq}}{\partial \beta}{\rm d}\beta\,. \tag{27}$$

Show that

$$\frac{\partial P_{\rm eq}}{\partial \alpha_i} = n_{{\rm eq},i} \quad \text{and} \quad \frac{\partial P_{\rm eq}}{\partial \beta} = -\beta\left[\rho_{\rm eq} + P_{\rm eq}\right] \tag{28}$$

and taking the differential of Eq. (26) conclude that

$${\rm d}\rho_{\rm eq} = \frac{1}{\beta}{\rm d}s + \beta \sum_i \alpha_i {\rm d}n_{{\rm eq},i}\,. \tag{29}$$

From the law of thermodynamics ${\rm d}\rho = T{\rm d}s + \sum_i \mu_i {\rm d}n_i$ with T the temperature of the bath and μ_i the chemical potential we can identify

$$\beta = \frac{1}{T} \quad \text{and} \quad \alpha_i = \frac{\mu_i}{T}\,. \tag{30}$$

In addition, for a, b, c, d in equilibrium, if $a + b \to c + d$, then the chemical potentials of these four species are related by

$$\mu_a + \mu_b = \mu_c + \mu_d\,. \tag{31}$$

In the standard model, because the photon number is not necessarily conserved, for instance in interactions such as $e^- + \gamma \to e^- + \gamma + \gamma$, their chemical potential is $\mu_\gamma = 0$. Moreover, as every standard model fermion ψ can annihilate with its anti-fermion $\overline{\psi}$ to produce photons, one concludes that $\mu_\psi = -\mu_{\overline{\psi}}$.

Exercise 4: Exercise

Show that in the ultra-relativistic limit (i.e., when $m_\psi \ll T$), $\mu_\psi = -\mu_{\overline{\psi}}$ implies

$$n_\psi - n_{\overline{\psi}} = \frac{g_f}{6\pi^2} T^3 \left[\pi^2 \left(\frac{\mu_\psi}{T}\right) + \left(\frac{\mu_\psi}{T}\right)^3\right] \tag{32}$$

One concludes that for $m \ll T$, if there are as many fermion ψ as anti-fermion $\overline{\psi}$ in the bath, then $\mu_\psi = 0$. At high temperature this is a good approximation for the standard model species and chemical potentials can be neglected.

Exercise 5: thermodynamics without chemical potential

Show that when $\mu = 0$, denoting $x = m_i/T$,

$$\begin{aligned} n_{\mathrm{eq},i}(t) &= \frac{g_{f,i}T^3}{2\pi^2}\sum_{n=1}^{\infty}\eta_i^{n+1}\frac{x^2}{n}K_2(xn) \\ \rho_{\mathrm{eq},i}(t) &= \frac{g_{f,i}T^4}{2\pi^2}\sum_{n=1}^{\infty}\eta_i^{n+1}\left\{\left(\frac{6x}{n^3}+\frac{x^3}{n}\right)K_1(xn)+\frac{3x^2}{n^2}K_0(xn)\right\} \\ P_{\mathrm{eq},i}(t) &= \frac{g_{f,i}T^4}{2\pi^2}\sum_{n=1}^{\infty}(-\eta_i)^{n+1}\frac{x^2}{n^2}K_2(xn)\,. \end{aligned} \tag{33}$$

Exercise 6: thermodynamics in the UR limit

Show that, the previous expressions (for $\mu = 0$) simplify in the ultra-relativistic limit to

$$\begin{cases} n_{\mathrm{eq}}(t) = \dfrac{g_f T}{\pi^2}\zeta(3)A \\ \rho_{\mathrm{eq}}(t) = \dfrac{g_f\pi^2 T^4}{30}B \\ P_{\mathrm{eq}}(t) = \dfrac{1}{3}\rho_{\mathrm{eq}}(t) \end{cases} \tag{34}$$

with $A = 1,\ B = 1$ for bosons, $A = 3/4,\ B = 7/8$ for fermions, and ζ the Riemann ζ-function.

Exercise 7: thermodynamics in the NR limit

Similarly, show that, in the non-relativistic limit (i.e., $m \gg T$)

$$\begin{cases} n_{\mathrm{eq}}(t) = g_f\left(\dfrac{mT}{2\pi}\right)^{3/2} e^{-\frac{(m-\mu)}{T}} \\ \rho_{\mathrm{eq}}(t) = m n_{\mathrm{eq}}(t) \end{cases} \tag{35}$$

For convenience we write the total energy density of the plasma in terms of an effective number of degree of freedom in the plasma, g_{eff}, such that

$$\rho_{\mathrm{eq}}(t) \equiv \frac{\pi^2 T^4}{30}g_{\mathrm{eff}}(T) \tag{36}$$

In the non-relativistic limit, both the number density and energy density are exponentially suppressed. Therefore, one can assume that species stop contributing to the energy density of the thermal bath as soon as they become non relativistic. We can then approximate g_{eff} and P_{eq} by

$$g_{\mathrm{eff}}(T) \sim \frac{30}{\pi^2 T^4}\sum_{i,\mathrm{UR}} B_i g_{f,i} \quad \text{and} \quad P_{\mathrm{eq}}(t) \sim \frac{\pi^2 T^4}{90}g_{\mathrm{eff}}(T) \tag{37}$$

which is a good approximation until neutrinos decouple from the plasma and thermalise to a temperature different to that of the primordial plasma. However, we will not enter into these details in this lecture as this is not crucial for the discussion of WIMP production. Similarly, as for a fluid at thermodynamical equilibrium, neglecting the chemical potentials of the ultra relativistic species the entropy density derived in Eq. (26) takes the form $s_{\mathrm{eq}} = (\rho_{\mathrm{eq}} + P_{\mathrm{eq}})/T$. We can, thus introduce a second definition for the effective number of degrees of freedom called h_{eff} as

$$s_{\mathrm{eq}} = \frac{2\pi^2}{45}h_{\mathrm{eff}}(T)T^3 \tag{38}$$

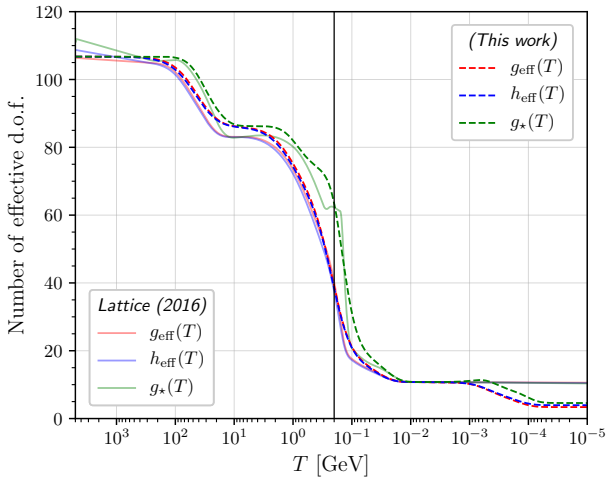

Figure 5: Number of effective degrees of freedom in the early Universe.

Finally, one also usually introduces $g_\star$ as

$$g_\star(T) \equiv \left[\frac{h_{\rm reff}(T)}{\sqrt{g_{\rm eff}(T)}}\left(1+\frac{\mathrm{d}\ln h_{\rm eff}(T)}{3\mathrm{d}\ln T}\right)\right]^2 , \tag{39}$$

which, in the case of an Universe with constant total entropy ($a^3 s_{\rm eq} = \text{cst}$) allows to relate the cosmic time t to the temperature T as

$$\frac{\mathrm{d}t}{\mathrm{d}T} = -\frac{1}{s_{\rm eq}}\sqrt{\frac{\pi}{45 G_{\rm N}}} g_\star^{1/2}(T)\,. \tag{40}$$

The three quantities $g_{\rm eff}$, $h_{\rm eff}$, and $g_\star$ are shown in figure 5 with the temperature of the plasma. Each breaks in the lines correspond to either a particle become non-relativistic when its mass gets smaller than the temperature, or to a phase transition. The most important one is the QCD phase transition, where massive mesons and baryons are formed and become non-relativistic. Moreover, note that $T \propto a^{-1}$ (the expansion rate of the Universe). Therefore, the entropy density roughly evolves as a^{-3}, that is, it simply dilutes in the expanding Universe as a number density would do. The energy density dilutes as a^{-4} because, on top of the volume expansion, the energy itself is reduced (think of it as a wavelength that is stretched).

> Remark: PBH formation In the introduction we mentionned PBH formation from the collapse of baryon overdensities in the early universe. This may particularly happens, if the overdensities are large enough, around the QCD phase transition where the huge drop in effective number of degree of freedom translates into a decrease of pressure, enabling the collapse.

In the following we now address the production of WIMPs via the vanilla freeze-out mechanism.

2.3 Dark matter production: chemical decoupling

We assume that WIMPs are produced from their interactions with the primordial plasma and have a mass $\sim$ GeV so that they quickly become non relativistic and their number density is exponentially suppressed. However, in order to produce enough WIMP to make the dark matter today the exponential suppression needs to stop. We say that the WIMPs need chemically decouple from the plasma or *freeze-out*, that is, the rate of creation and annihilation of WIMPs is suppressed. The precise moment the decoupling happens fixes the final density of WIMPs and depends on the strength of the coupling in comparison to the expansion rate which dilutes the plasma. Due to

their large mass we can safely assume that the WIMPs decouple once non-relativistic. Moreover, we usually assume that although they decouple chemically, they stay in thermal contact with the plasma, that is, scattering interactions are still efficient. This is a good approximation if not in specific scenarios.

2.3.1 The collision operator

Let us assume that the WIMPs χ, are produced from the creation and annihilation processes $\chi(1)+\overline{\chi}(2) \leftrightarrow \psi(3)+\overline{\psi}(4)$ where ψ are standard model fermions (generalisation to standard model bosons is straightforwards but requires the addition of symmetry factors to avoid double counting). The collision operator for the dark matter PSDF, f_χ, as appearing in Eq. (21) is then

$$C[f_\chi](p_1) = \frac{1}{2g_\chi}\int \left\{\mathcal{F}_{\psi\bar{\psi}\to\chi\bar{\chi}}(p_i^\mu)|\mathcal{M}_{\to}|^2 - \mathcal{F}_{\chi\bar{\chi}\to\psi\bar{\psi}}(p_i^\mu)|\mathcal{M}_{\leftarrow}|^2\right\} \mathrm{d}\overline{\Pi}_{\mathrm{LIPS}} \tag{41}$$

where the integration volume element is the Lorentz-invariant phase space

$$\mathrm{d}\overline{\Pi}_{\mathrm{LIPS}} = (2\pi)^4\delta^{(4)}\left(p_1^\mu + p_2^\mu - p_3^\mu - p_4^\mu\right)\prod_{i=2}^{4}\frac{1}{2E_i(p_i)}\frac{\mathrm{d}\mathbf{p}_i^3}{(2\pi)^3}\,. \tag{42}$$

> Remark: The expressions, because obtained from quantum field theory, should only be valid in the locally inertial frame. Nonetheless, as the FLRW metric corresponds to a conformal transformation of Minkowski's, the equations remain valid in FLRW too.

In addition, in this expression we have introduced phase space factors

$$\begin{aligned}\mathcal{F}_{\chi\bar{\chi}\to\psi\bar{\psi}}(p_i^\mu) &\equiv f_\chi(t,p_1^\mu)f_{\bar{\chi}}(t,p_2^\mu)\left[1+\eta_\psi f_\psi(t,p_3^\mu)\right]\left[1+\eta_\psi f_{\bar{\psi}}(t,p_4^\mu)\right]\\ \mathcal{F}_{\psi\bar{\psi}\to\chi\bar{\chi}}(p_i^\mu) &\equiv f_\psi(t,p_3^\mu)f_{\bar{\psi}}(t,p_4^\mu)\left[1-f_\chi(t,p_1^\mu)\right]\left[1-f_{\bar{\chi}}(t,p_2^\mu)\right]\end{aligned} \tag{43}$$

as well as the spin-summed matrix elements

$$\begin{aligned}|\mathcal{M}_{\to}|^2 &\equiv \prod_{i=1}^{4}\sum_{s_i}|\mathcal{M}_{\psi\bar{\psi}\to\chi\bar{\chi}}|^2\\ |\mathcal{M}_{\leftarrow}|^2 &\equiv \prod_{i=1}^{4}\sum_{s_i}|\mathcal{M}_{\chi\bar{\chi}\to\psi\bar{\psi}}|^2\,.\end{aligned} \tag{44}$$

In the case of a CP-invariant interaction then the two matrix elements are equal $|\mathcal{M}_{\leftrightarrow}|^2 \equiv |\mathcal{M}_{\to}|^2 = |\mathcal{M}_{\leftarrow}|^2$ and we can rewrite the collision term as

$$C[f_\chi](p_1) = \frac{1}{2g_{f,\chi}}\int |\mathcal{M}_{\leftrightarrow}|^2\left\{\mathcal{F}_{\psi\bar{\psi}\to\chi\bar{\chi}}(p_i^\mu) - \mathcal{F}_{\chi\bar{\chi}\to\psi\bar{\psi}}(p_i^\mu)\right\}\mathrm{d}\overline{\Pi}_{\mathrm{LIPS}}\,. \tag{45}$$

Integrating over the momentum p_χ^μ and simplifying the phase space factors because the WIMPs decouple while non relativistic, we obtain

$$g_{f,\chi}\int C[f_\chi](p_1)\frac{p_1^2}{E_1(p_1)}\frac{\mathrm{d}p_1}{2\pi^2} = \left\langle\sigma_{\chi\bar{\chi}\to\psi\bar{\psi}}v_{\mathrm{M\o l}}\right\rangle_{\mathrm{eq}}\left(n_{\mathrm{eq},\chi}n_{\mathrm{eq},\bar{\chi}} - n_\chi n_{\bar{\chi}}\right)\,. \tag{46}$$

where the *thermally-averaged* cross section is defined by

$$\left\langle\sigma_{\chi\bar{\chi}\to\psi\bar{\psi}}v_{\mathrm{M\o l}}\right\rangle_{\mathrm{eq}} \equiv \frac{g_{f,\chi}g_{f,\bar{\chi}}}{n_{\mathrm{eq},\chi}n_{\mathrm{eq},\bar{\chi}}}\int \sigma_{\chi\bar{\chi}\to\psi\bar{\psi}}v_{\mathrm{M\o l}}\exp\left(\frac{E_\chi(p_1)+E_{\bar{\chi}}(p_2)}{T}\right)\frac{\mathrm{d}^3\mathbf{p}_1}{(2\pi)^3}\frac{\mathrm{d}^3\mathbf{p}_2}{(2\pi)^3}\,, \tag{47}$$

and the Møller velocity is

$$v_{\text{Møl}} \equiv \frac{1}{E_\chi(p_1)E_{\bar{\chi}}(p_2)}\sqrt{(p_1^\mu p_{2,\mu})^2 - m_\chi^2 m_{\bar{\chi}}^2}\,. \tag{48}$$

> Remark: the Boltzmann equation is only *semi-classical*. Even though the collision operator includes Pauli-blocking and Bose enhancement factors, some ambiguities are left when counting interactions. For instance a $2 \to 2$ interaction $a+b \to c+d$, can effectively be counted as $a+b \to c$ on the one hand, $c \to d+e$ on the other hand, but also directly as $a+b \to$ (offshell c) $\to d+e$. A precise (and much more involved) quantum description of the system is possible through the Kadanoff- Baym equation, based on the density matrix. However, in a cosmological context, this framework is mostly relevant to study leptogenesis and baryogenesis

2.3.2 Chemical decoupling

The total dark matter density is denoted by n_{DM}. Two scenarios are possible, either the WIMP is its own antiparticle, a Majorana fermion, or a Dirac fermion. In the Majorana case we have $n_{\text{DM}} = n_\chi = n_{\bar{\chi}}$. In the Dirac case, then $n_{\text{DM}} = n_\chi + n_{\bar{\chi}}$. The master equation for chemical decoupling is obtained from Eqs. (21, 46). For Majorana WIMPs, it simply yields

$$\frac{\mathrm{d}n_{\text{DM}}}{\mathrm{d}t} + 3Hn_{\text{DM}} = \left\langle \sigma_{\chi\chi\to\psi\bar{\psi}} v_{\text{Møl}} \right\rangle_{\text{eq}} \left(n_{\text{eq,DM}}^2 - n_{\text{DM}}^2\right) \quad \text{(Majorana)} \tag{49}$$

For Dirac WIMPs it is slightly different as we need to sum over the contribution of the particles and antiparticles. In full generality one then have a system of two coupled equations. However, assuming that $n_\chi = n_{\bar{\chi}}$ we obtain a similar expression with an extra factor 1/2,

$$\frac{\mathrm{d}n_{\text{DM}}}{\mathrm{d}t} + 3Hn_{\text{DM}} = \frac{1}{2}\left\langle \sigma_{\chi\bar{\chi}\to\psi\bar{\psi}} v_{\text{Møl}} \right\rangle_{\text{eq}} \left(n_{\text{eq,DM}}^2 - n_{\text{DM}}^2\right) \quad \text{(Dirac)} \tag{50}$$

(a factor 1/4 comes from $n_{\text{DM}}^2 = n_\chi^2/4$ and a factor 2 comes from the addition of the equation for n_χ to that for $n_{\bar{\chi}}$). In the following we will consider the case of Majorana particles for simplicity. In this master equation appears a clear competition between the expansion rate of the Universe H and the annihilation rate of the dark matter particles

$$\Gamma_{\text{ann}} \equiv \left\langle \sigma_{\chi\chi\to\psi\bar{\psi}} v_{\text{Møl}} \right\rangle_{\text{eq}} n_{\text{DM}}\,. \tag{51}$$

When Γ_{ann} dominates the number density goes to the equilibrium density, that is depleted by an exponential suppression factor (as the WIMP is non relativistic). When H dominates, the equation becomes that of a simple dilution and $n_{\text{DM}} \propto a^{-3}$. Chemical decoupling roughly occurs when these two quantities are equal to each other. We transition from a regime of exponential suppression to a regime of simple dilution, the dark matter density *freezes out*.

To numerically solve the master equation, it is, however, better to change variables. We usually define the dark matter yield as the ratio

$$Y_{\text{DM}} \equiv \frac{n_{\text{DM}}}{s_{\text{eq}}} \tag{52}$$

where s is the entropy density. Indeed, recall that s_{eq} approximately goes as a^{-3}, thus, after the decoupling Y_χ goes to a constant value. Moreover, we change variables from the cosmic time t that is difficult to make sense of at this early time of the Universe to $x \equiv m_{\text{DM}}/T$ with m_{DM} the dark matter mass.

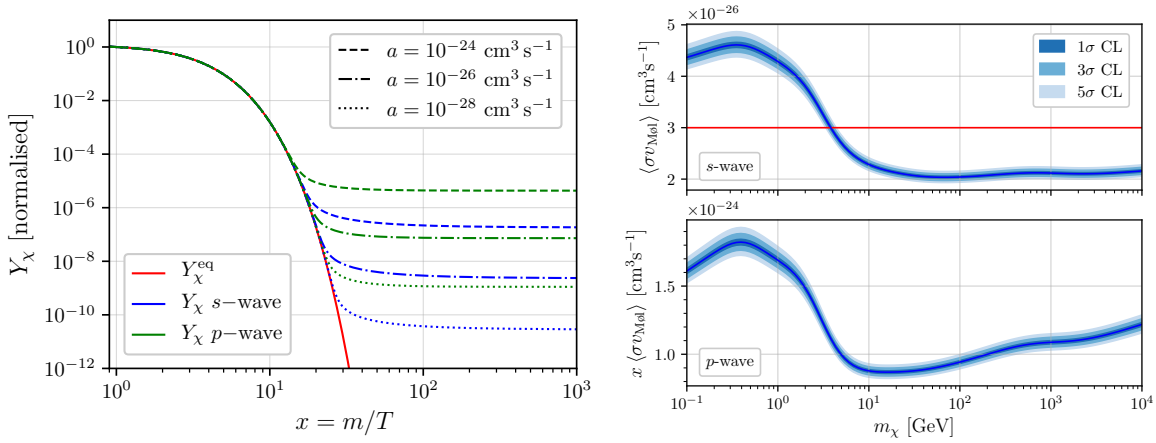

Figure 6: **Left panel.** Normalised dark matter yield for a cross section $\sigma v_{\rm Møl} = a x^{-n}$ with $n = 0$ (resp $n = 1$) for s- (resp.) p-wave. Different values of a are shown and the equilibrium yield is given in red. **Right panel.** Value of the s- (upper) and p-wave (lower) thermally averaged cross-section that produces the correct abundance in terms of the dark matter mass. The usually adopted value is shown in red.

> Exercise 8: Differential equation for the dark matter yield
>
> Show that the differential equation for the dark matter yield in terms of the variable x is
>
> $$\frac{{\rm d}Y_{\rm DM}}{{\rm d}x} = \sqrt{\frac{\pi}{45 G_{\rm N}}} \frac{m_{\rm DM}}{x^2} g_\star^{1/2} \left(\frac{m_{\rm DM}}{x}\right) \left\langle \sigma_{\chi\chi\to\psi\bar{\psi}} v_{\rm Møl} \right\rangle_{\rm eq} \left(Y_{\rm eq,DM}^2 - Y_{\rm DM}^2\right) , \tag{53}$$

Numerically solving this equation from $x = 1$, when the WIMP becomes non relativistic, with $Y_{\rm DM}(x = 1) = Y_{\rm eq,DM}$ gives the dark matter yield today $Y_{\rm DM,0}$ and therefore the current abundance

$$\Omega_{\rm DM,0} h^2 = \frac{m_{\rm DM} s_{\rm eq}(t_0)}{\rho_{\rm c,0}} Y_{\rm DM,0} h^2 \sim 2.8 \times 10^8 \times Y_{\rm DM,0} \left(\frac{m_{\rm DM}}{\rm GeV}\right) . \tag{54}$$

In practice, unless we hit a resonance, the thermally averaged cross-section can be expanded as $\left\langle \sigma_{\chi\chi\to\psi\bar{\psi}} v_{\rm Møl} \right\rangle_{\rm eq} = \sigma_0 + \sigma_1/x + \sigma_2/x^2 \ldots$. This decomposition is called the partial wave decomposition and σ_0, σ_1, σ_2 are respectively referred to as the s-, p-, and d-wave annihilation cross-sections. In practice we only consider $x > 1$ as the WIMPs decouple while non relativistic and we find that decoupling actually happens around $x \sim 25$. If σ_0 is non zero it most likely dominates the cross section. If $\sigma_0 = 0$ and $\sigma_1 \neq 0$ the latter dominates. Thus, we usually solve this equation for the s- and p- wave scenario (which often arise in real particle models as we will see below) separately. In figure 6 we show the evolution of the dark matter yield with x for various scenarios on the left panel. In addition, on the right panel we display the ralue of the s- (upper) and p-wave (lower) thermally averaged cross-section that produces the correct abundance in terms of the dark matter mass. This first shows that decoupling indeed occurs for $x \sim 25$ and that this is not very sensitive to the model parameters. Secondly, the correct abundance in the s-wave case is reached for an almost constant cross-section usually taken to be 3×10^{-26} cm s^{-1}. Actually, above a few GeV the true value is slightly smaller and below one GeV it is higher. The mass threshold, which appears for $m_{\rm DM} \sim 25 \times \Lambda_{\rm QCD}$, is due to the QCD phase transition brutally changing the effective number of degrees of freedom.

> Exercise 9: Back of the envelop estimate for freeze-out
>
> Let us assume a s-wave cross-section $\left\langle \sigma_{\chi\chi\to\psi\bar{\psi}} v_{\rm Møl} \right\rangle_{\rm eq} = \sigma_0$, independent of x. After chemical

decoupling show that the yields evolves as

$$\frac{\mathrm{d}Y_{\mathrm{DM}}}{\mathrm{d}x} = \sqrt{\frac{\pi}{45G_{\mathrm{N}}}} \frac{m_{\mathrm{DM}}}{x^2} g_\star^{1/2} \left(\frac{m_{\mathrm{DM}}}{x}\right) Y_{\mathrm{DM}}^2 \,, \tag{55}$$

Conclude that

$$Y_{\mathrm{DM},0} \sim \sqrt{\frac{45G_{\mathrm{N}}}{\pi}} \left\langle g_\star^{1/2} \right\rangle \frac{x_{\mathrm{f}}}{m_{\mathrm{DM}}\sigma_0} \tag{56}$$

with x_{f} the value of x at freeze out and $\left\langle g_\star^{1/2} \right\rangle$ a *mean* value of $g_\star^{1/2}$ from freeze-out to today.

Exercise 10: The WIMP miracle

Plug in numbers and prove that

$$\Omega_{\mathrm{DM},0}h^2 \sim 0.1 \left(\frac{x_{\mathrm{f}}}{25}\right) \left\langle g_\star^{1/2} \right\rangle \left(\frac{10^{-8}\ \mathrm{GeV}^{-2}}{\sigma_0}\right) . \tag{57}$$

Therefore, for a cross-section of the electroweak scale $\sigma \sim 10^{-8}\ \mathrm{GeV}^{-2} \sim 10^{-25}\ \mathrm{cm}^3\,\mathrm{s}^{-1}$, we obtain the correct dark matter abundance. Note that for a back of the envelop estimate, the orders of magnitudes are in agreement with the full computation. This *coincidence*, called the WIMP miracle has been one of the strongest motivations to search for WIMPs in the last decades. In order to go in better detail into those calculations let us go through an example below.

2.4 Example: from the scalar portal model to simplified models

For this example we follow [Lopez-Honorez et al., 2012]. In this model let us consider that the dark matter is a Majorana fermion $\chi = \psi_{\chi,\mathrm{L}} + \psi^c_{\chi,\mathrm{L}}$ (in 4-component notation in the chiral basis) where $\psi_{\chi,\mathrm{L}}$ is a left handed Weyl fermion $\psi_{\chi,\mathrm{L}} = (\chi_{\mathrm{L}}\ 0)^T$ and we recall that $\psi^c_{\chi,\mathrm{L}} \equiv \gamma^0 C \psi^*_{\chi,\mathrm{L}} = (0\ i\sigma^2\psi^*_{\chi,\mathrm{L}})^T$ with $C = i\gamma^2\gamma^0$ the charge conjugation matrix. Note that a direct property of C is that $\gamma^0 C(\gamma^0 C)^* = 1$ such that $(\psi^c_{\chi,\mathrm{L}})^c = \psi_{\chi,\mathrm{L}}$ and χ is indeed a Majorana Fermion. The interactions between dark matter and the standard model interaction are mediated by a real scalar singlet φ mixing with the Brout-Englert-Higgs (BEH) doublet H. Let us start with the standard model Lagrangian to which we add a dark sector

$$\mathcal{L} \ni \mathcal{L}_\chi + \mathcal{L}_\varphi + \mathcal{L}_H - V_{\varphi H}(\varphi, H^\dagger H) \tag{58}$$

where the different parts for the dark matter sector, the scalar singlet sector and the BEH doublet sector are respectively given by

$$\begin{cases} \mathcal{L}_\chi = \dfrac{1}{2}\left[\chi_{\mathrm{L}}^\dagger \overline{\sigma}^\mu \partial_\mu \chi_{\mathrm{L}} - (\mu_\chi + g\varphi)\chi_{\mathrm{L}}^\dagger i\sigma^2 \chi_L^\star + \mathrm{h.c.}\right] , \\ \mathcal{L}_\varphi = \dfrac{1}{2}\partial_\mu\varphi\partial^\mu\varphi - V_\varphi(\varphi) \,, \\ \mathcal{L}_H = (D_\mu H)^\dagger D^\mu H - V_H(H^\dagger H) + \mathcal{L}_{\mathrm{Yukawa}} \,. \end{cases} \tag{59}$$

where the covariant derivative is that of the standard model $D_\mu \equiv \partial_\mu - ig_W W^i_\mu \sigma^i/2 - ig'_W B_\mu/2$. The Yukawa Lagrangian is the usual standard model one, coupling the BEH doublet to the fermions. Note that, here, g and μ_χ can be complex numbers. In addition, the total scalar potential is

$$V(\varphi, H^\dagger H) = V_\varphi(\varphi) + V_H(H^\dagger H) + V_{\varphi H}(\varphi, H^\dagger H) \tag{60}$$

with each part being

$$\begin{cases} V_\varphi(\varphi) = -\dfrac{\mu_\varphi^2}{2} + \dfrac{\lambda_\varphi}{4}\varphi^4\,, \\ V_H(H^\dagger H) = -\mu_H^2 H^\dagger H + \lambda_H (H^\dagger H)^2\,, \\ V_{\varphi H}(\varphi, H^\dagger H) = \left(\dfrac{\lambda_4}{2}\varphi^2 + \mu\varphi\right) H^\dagger H\,. \end{cases} \tag{61}$$

The coupling of the dark sector (made of χ and φ) to the standard model is encoded into $V_{\varphi H}$ mixing the two scalar sectors. Assuming that H and φ acquire a VEV, respectively denoted v_1 and v_2, we develop the expression in the unitary gauge such that after symmetry breaking

$$H \to \frac{1}{\sqrt{2}}\begin{pmatrix} 0 \\ v_1 + h \end{pmatrix} \quad \text{and} \quad \varphi \to v_2 + \phi\,, \tag{62}$$

with the condition on the VEVs (obtained searching for the minimum of the pontential)

$$\begin{cases} -\mu_\varphi^2 + \lambda_\varphi v_2^2 + \dfrac{\lambda_4}{2} v_1^2 + \dfrac{\mu}{2}\dfrac{v_1^2}{v_2} = 0 \\ -\mu_H^2 + \lambda_H v_1^2 + \dfrac{\lambda_4}{2} v_2^2 + \mu v_2 = 0 \end{cases}. \tag{63}$$

There are then two important points in the model. Firstly, the VEV of φ contributes to a mass term for the dark matter and the complex nature of the coupling g allows for both scalar and pseudo scalar interactions with ϕ. Secondly, due to non diagonal mass terms in the potential ϕ and h will be mixed, hence providing interaction channels between the dark matter and the standard model fermions. We detail these two points in the following.

2.4.1 The dark matter sector

The dark matter sector of the Lagrangian is given in two-component notations. We can however rewrite it in 4-component notation, e.g., for the kinetic term as asked in the exercise below.

> Exercise 11: Kinetic term for dark matter
>
> Show that we can rewritte the kinetic term in 4-component notation as
>
> $$\frac{1}{2}\left[\chi_{\rm L}^\dagger \overline{\sigma}^\mu \partial_\mu \chi_{\rm L} + \text{h.c.}\right] = \frac{1}{2}\overline{\chi} i\partial\!\!\!/ \chi \tag{64}$$

After symmetry breaking, the Lagrangian of the dark matter sector becomes

$$\begin{aligned} \mathcal{L}_\chi &= \frac{1}{2}\overline{\chi} i\partial\!\!\!/ \chi - \frac{1}{2}\left[(\mu_\chi + g v_2 + g\phi)\chi_{\rm L}^\dagger i\sigma^2 \chi_{\rm L}^* + \text{h.c.}\right] \\ &= \frac{1}{2}\overline{\chi} i\partial\!\!\!/ \chi - \frac{1}{2}|\mu_\chi + g v_2|\left[\chi_{\rm L}^\dagger i\sigma^2 \chi_{\rm L}^* e^{i\alpha} + \text{h.c.}\right] - \frac{1}{2}\phi\left[g\chi_{\rm L}^\dagger i\sigma^2\chi_{\rm L}^* + \text{h.c.}\right] \end{aligned} \tag{65}$$

with $\alpha = \arg(\mu_\chi + g v_2)$. The second term is a mass term for the dark matter field while the last one is the interaction term between the dark matter and the singlet scalar. In order to have a real mass term we can transform $\chi_{\rm L}$ by the chiral rotation $\chi_{\rm L} \to e^{i\alpha/2}\chi_{\rm L}$, one then also transforms $\chi^* \to e^{-i\alpha/2}\chi_{\rm L}^*$ and $\chi^\dagger \to e^{-i\alpha/2}\chi_{\rm L}^\dagger$. Note that is correspond to $\chi \to e^{-i\alpha/2\gamma^5}\chi$ in 4-component notation. Moreover, the chiral phase rotation leaves the kinetic term invariant. Therefore, after this rotation the phase term disappears and

$$\mathcal{L}_\chi \to \frac{1}{2}\overline{\chi} i\partial\!\!\!/ \chi - \frac{1}{2}|\mu_\chi + g v_2|\left[\chi_{\rm L}^\dagger i\sigma^2\chi_{\rm L}^* + \text{h.c.}\right] - \frac{1}{2}\phi\left[g e^{-i\alpha}\chi_{\rm L}^\dagger i\sigma^2\chi_{\rm L}^* + \text{h.c.}\right]. \tag{66}$$

where we can identify $m_\chi = |\mu_\chi + g v_2|$.

Exercise 12: Some algebra with fermions

Show that

$$\begin{cases} \overline{\chi}\chi & = \left[\chi_{\mathrm{L}}^{\dagger} i\sigma^2 \chi_{\mathrm{L}}^{*} + \mathrm{h.c.}\right] = \chi_{\mathrm{L}}^{\dagger} i\sigma^2 \chi_{\mathrm{L}}^{*} - \chi_{\mathrm{L}}^{\mathrm{T}} i\sigma^2 \chi_{\mathrm{L}} \\ \overline{\chi}\gamma^5\chi & = \left[\chi_{\mathrm{L}}^{\dagger} i\sigma^2 \chi_{\mathrm{L}}^{*} - \mathrm{h.c.}\right] = \chi_{\mathrm{L}}^{\dagger} i\sigma^2 \chi_{\mathrm{L}}^{*} + \chi_{\mathrm{L}}^{\mathrm{T}} i\sigma^2 \chi_{\mathrm{L}} \end{cases} \tag{67}$$

Exercise 13: Interaction term

From the result of the previous exercise, show that

$$\begin{aligned} \left[g e^{-i\alpha} \chi_{\mathrm{L}}^{\dagger} i\sigma^2 \chi_{\mathrm{L}}^{*} + \mathrm{h.c.}\right] &= \overline{\chi}\chi \left(\frac{g e^{-i\alpha} + g^* e^{i\alpha}}{2}\right) + \overline{\chi}\gamma^5\chi \left(\frac{g e^{-i\alpha} - g^* e^{i\alpha}}{2}\right) \\ &= \mathrm{Re}\left(g e^{-i\alpha}\right) \overline{\chi}\chi + i\mathrm{Im}\left(g e^{-i\alpha}\right) \overline{\chi}\gamma^5\chi \end{aligned} \tag{68}$$

Let us denote $g_{\mathrm{s}} = \mathrm{Re}\left(g e^{-i\alpha}\right)$ and $g_{\mathrm{p}} = \mathrm{Im}\left(g e^{-i\alpha}\right)$ where s stands for scalar and p for pseudo-scalar coupling. The Lagrangian for the dark matter sector, after spontaneous symmetry breaking and after performing a chiral rotation of the field becomes (using the same name for that transformed Lagrangian for simplicity),

$$\mathcal{L}_{\chi} = \frac{1}{2}\overline{\chi} i\partial\!\!\!/ \chi - \frac{1}{2}\left[m_{\chi}\overline{\chi}\chi + g_{\mathrm{s}}\phi\overline{\chi}\chi + i g_{\mathrm{p}}\phi\overline{\chi}\gamma^5\chi\right] . \tag{69}$$

2.4.2 Scalar sector and portal

After symmetry breaking the potential transforms to $V(\varphi, H) \to V(\phi, h)$ (for simplicity we call the two potential by the same later, with the convention that for now on we will always refer to the potential after symmetry breaking. The mass part of the potential can be written

$$V(\phi, h) \ni \frac{1}{2}\begin{pmatrix} h & \phi \end{pmatrix} \mathcal{M} \begin{pmatrix} h \\ \phi \end{pmatrix} \tag{70}$$

with the mass matrix

$$\mathcal{M} = 2\begin{pmatrix} -\mu_H^2 + 3\lambda_H v_1^2 + \dfrac{\lambda_4}{2} v_2^2 + \mu v_2 & \lambda_4 v_1 v_2 + \mu v_1 \\ \lambda_4 v_1 v_2 + \mu v_1 & -\mu_\varphi^2 + 3\lambda_\varphi v_2^2 + \dfrac{\lambda_4}{2} v_1^2 \end{pmatrix} . \tag{71}$$

The latter is diagonalised by the change of base matrix $\mathcal{P}$ such that such that $\mathcal{P}^{-1}\mathcal{M}\mathcal{P} = \mathcal{D}$ with $\mathcal{D}$ diagonal. More precisely, the change of base matrix takes the form

$$\mathcal{P} = \begin{pmatrix} \cos\theta & -\sin\theta \\ \sin\theta & \cos\theta \end{pmatrix} \quad \text{with} \quad \theta \in [0, \pi[. \tag{72}$$

Exercise 14: Mass diagonalisation

Show that the angle θ satisfies

$$\tan 2\theta = \frac{2\mu v_1 + 2\lambda_4 v_1 v_2}{\mu_\varphi^2 - \mu_H^2 + 3(\lambda_H v_1^2 - \lambda_\varphi v_2^2) + \dfrac{\lambda_4}{2}(v_2^2 - v_1^2) + \mu v_2} . \tag{73}$$

Using Eq. (63) simplify the expression of $\tan 2\theta$ to

$$\tan 2\theta = \frac{\mu v_1 + \lambda_4 v_1 v_2}{\lambda_H v_1^2 - \lambda_\varphi v_2^2 + \frac{\mu v_1^2}{4 v_2}} \,. \tag{74}$$

Let us call h_1 and h_2 the two mass eigenstates, then

$$\begin{pmatrix} h_1 \\ h_2 \end{pmatrix} = \mathcal{P}^{-1} \begin{pmatrix} h \\ \phi \end{pmatrix} \tag{75}$$

and we place ourselves in the regime $\theta \ll 1$ such that $m_{h_1} \sim m_h \sim 125$ GeV is the Higgs discovered at the LHC. Therefore, after spontaneous symmetry breaking the Lagrangian has the terms (amongst many other not relevant for the discussion and therefore not mentioned)

$$\begin{aligned} \mathcal{L} \ni & \frac{1}{2}\partial_\mu h_1 \partial^\mu h_1 + \frac{1}{2}\partial_\mu h_2 \partial^\mu h_2 - \frac{1}{2} m_{h_1} h_1^2 - \frac{1}{2} m_{h_2} h_2^2 + \frac{1}{2}\overline{\chi} i \partial\!\!\!/ \chi - \frac{1}{2} m_\chi \overline{\chi}\chi \\ & - \frac{1}{2}(\sin\theta h_1 + \cos\theta h_2)\left[g_{\rm s} \overline{\chi}\chi + i g_{\rm p} \overline{\chi}\gamma^5 \chi \right] \\ & + (\cos\theta h_1 - \sin\theta h_2)\left[m_Z^2 v_1 Z_\mu Z^\mu + 2 m_W^2 v_1 W_\mu^+ W^{-\mu} - \sum_f \frac{m_f}{v_1} \overline{f} f \right] \end{aligned} \tag{76}$$

where the sum runs over all massive standard model fermions with mass m_f. The coupling of the dark sector to the standard model is now explicit from the second line and third. In the following we now address the phenomenological study of this model by means of simplified models.

2.4.3 Using simplified models

While studying the full UV complete model as we have done before informs us about the underlying relationships between the parameters and provide a consistent framework, this hard work is not always necessary when we focus on the phenomenology. From now on, we only consider the interaction terms of the Lagrangian. We can simply treat the full model as a fermionic Majorana dark matter with scalar and pseudo scalar interactions to two scalar fields h_1 and h_2, themselves interacting with the standard model particles. For simplicity we will focus on the interaction with standard model fermions. Obviously the interactions with the Z and W bosons as well as that with photons and gluons at loop level are important for a full phenomenological study, however, this is beyound the scope of this lecture. Therefore let us restrict the interaction Lagrangian to

$$\mathcal{L}_{\rm int} = -\frac{1}{2}(\sin\theta h_1 + \cos\theta h_2)\left[g_{\rm s} \overline{\chi}\chi + i g_{\rm p} \overline{\chi}\gamma^5 \chi \right] - (\cos\theta h_1 - \sin\theta h_2) \sum_f \frac{m_f}{v_1} \overline{f} f \tag{77}$$

In a more concise framework, we can write the interaction Lagrangian as

$$\mathcal{L}_{\rm simp} = -\sum_j \left\{ \frac{1}{2}\rho_j \left[g^j_{\rho\chi,{\rm s}} \overline{\chi}\chi + i g^j_{\rho\chi,{\rm p}} \overline{\chi}\gamma^5\chi \right] + \rho_j \sum_f g^j_{\rho f} \overline{f} f \right\} \tag{78}$$

with couplings depending on θ, $g_{\rm s}$, $g_{\rm p}$, m_f, and v_1. Such a Lagrangian is referred to as a s-channel simplified model (s-channel meaning that the only interactions ar of the type two dark matter field with one mediator or two standard model fermion fields with one mediator). Simplified model are often used in the literature to place generic constraints that can then be applied to UV-complete models. Here the simplified model is nonetheless non trivial has it contains two mediators with, a priori, different mass. Note that because $\bar{\psi}\psi$ is CP-even while $\bar{\psi}\gamma^5\psi$ is CP-odd the model cannot be, in general, CP-invariant. Nonetheless, we can still compute the cross-section for annihilation into a pair of standard model fermions. This is the goal of the following exercise.

Exercise 15: annihilation cross-section

Show that the cross-section of the annihilation $\chi\chi \to f\overline{f}$ takes the form (be careful as we are working with Majorana particles)

$$\begin{aligned}\sigma_{\chi\chi\to f\overline{f}}(s) =& \frac{m_\chi^4 m_f^2}{16\pi s v_1^2}\sin^2 2\theta \left\{\sum_{j=1,2}\frac{1}{(s-m_j^2)^2+m_j^2\Gamma_j^2} + \text{c.t.}\right\} \\ &\times \left[g_\text{s}^2\,(S-1)^{1/2}\left(S-\frac{m_f^2}{m_\chi^2}\right)^{3/2} + g_\text{p}^2 S^2\,(S-1)^{-1/2}\left(S-\frac{m_f^2}{m_\chi^2}\right)^{1/2}\right]\end{aligned} \tag{79}$$

where $S \equiv s/(4m_\chi^2)$ with s the Mandelstam variable. In addition, c.t. refers to a cross-term that is long and unimportant for the discussion, so left out. Note, however, that there are no cross-terms between the scalar and pseudo-scalar coupling (only between scalar and scalar, and pseudo-scalar and pseudo-scalar).

The first part of the equation is due to the scalar coupling while the second part is due to the pseudo scalar coupling. In addition, at low velocity (small s) we can expand

$$S = \frac{s}{4m_\chi^2} \sim 1 + \frac{v_\text{Møl}^2}{4} \tag{80}$$

Moreover, for the chemical decoupling, as the dark matter remains in thermal equilibrium $T \propto m_\text{DM} v_\text{Møl}^2$ and the variable x satisfies $x \sim v_\text{Møl}^{-2}$. Thus, the cross scalar and pseudo-scalar part of the cross section respectively satisfy

$$\begin{cases} v_\text{Møl}\sigma^\text{scalar}_{\chi\chi\to f\overline{f}}(s) \propto v_\text{Møl}^2 \propto 1/x \\ v_\text{Møl}\sigma^\text{pseudo-scalar}_{\chi\chi\to f\overline{f}}(s) \propto \text{cst}\,. \end{cases} \tag{81}$$

Said differently we find out that the scalar interaction give rise to a p-wave cross section that is velocity suppressed while the pseudo-scalar interaction produces a s-wave cross-section.

Remark: Because the difference between s- or p-wave amounts to a velocity suppression factors, this has a huge impact on the indirect detection limits we can set. Indeed if the dark matter annihilates with a p-wave annihilation cross-section, higher couplings (in comparison to the s-wave case) are necessary to compensate the velocity suppression of the non relativistic dark matter at decoupling. Indeed, the subsequent higher cross-section maintains chemical contact with the thermal bath long enough not to overclose the Universe. Today, however, the dark matter is much slower than what it was at decoupling and the suppression factor is thus much stronger. Therefore, it is much more difficult to set constraints on the p-wave annihilation cross-section that give the right DM abundance.

2.4.4 Effective field theory

Another degree of simplification would be to use effective field theory, that is define the Lagrangian with dimension 6 operators, integrating out the mediator(s),

$$\mathcal{L}_\text{EFT} = \frac{g_\text{s} m_f \sin 2\theta}{2v_1\Lambda_\text{s}^2}(\overline{\chi}\chi)(\overline{f}f) + \frac{g_\text{p} m_f \sin 2\theta}{2v_2\Lambda_\text{p}^2}(i\overline{\chi}\gamma^5\chi)(\overline{f}f) \tag{82}$$

If the mass of the mediators are much larger than the energy scale we are interested in, this is a good approximation and to match the previous the mass scale would be

$$\Lambda_\text{s} \sim \Lambda_\text{p} \sim \left(\frac{1}{m_{h_1}^4} + \frac{1}{m_{h_2}^4}\right)^{-1/4}. \tag{83}$$

Therefore, any constraints in the effective couplings can be translated as degenerate constraints on all the parameters. This makes the effective field theory approach very efficient to make generic statements, even though one should always keep in mind that its results are not valid on the entire parameter range (on resonance for instance, etc.).

2.5 A few more comments

- In the case of FIMPs we can use a similar formalism, except that the initial condition is $Y_{\rm DM} = 0$ instead of $Y_{\rm DM} = Y_{\rm DM,eq}$ as the coupling are too small to reach thermal equilibrium with the primordial plasma in the first place.
- Additionally to chemical decoupling, WIMP also kinetically decouple (that is loose the thermal contact and acquire their own temperature which evolves differently to that of the bath). Usually, kinetic decoupling happens well after chemical decoupling (the assumption made here) and is maintained by elastic scatterings with standard model particles at a frequency that is proportional to their density in the bath (while for chemical decoupling the frequency of annihilations is proportional to the dark matter density in the bath $\Gamma_{\rm ann} = n_\chi \langle \sigma v \rangle$).
- The kinetic decoupling scale fixes the free-streaming distance the WIMP can travel and thus, the size of the lightest structures it may form.
- The scattering interactions ensuring thermal contact are the same that are probed by direct experiments today. Therefore, chemical decoupling and indirect detection are driven by the same interactions and same is for kinetic decoupling and direct detection. In this scenario, probing dark matter today is thus equivalent to directly probe its formation mechanism.

References

[Abbott et al., 2019] Abbott, B. P. et al. (2019). GWTC-1: A Gravitational-Wave Transient Catalog of Compact Binary Mergers Observed by LIGO and Virgo during the First and Second Observing Runs. *Phys. Rev. X*, 9(3):031040.

[Aghanim et al., 2020] Aghanim, N. et al. (2020). Planck 2018 results. I. Overview and the cosmological legacy of Planck. *Astron. Astrophys.*, 641:A1.

[Aker et al., 2022] Aker, M. et al. (2022). Direct neutrino-mass measurement with sub-electronvolt sensitivity. *Nature Phys.*, 18(2):160–166.

[Aprile et al., 2020] Aprile, E. et al. (2020). Excess electronic recoil events in XENON1T. *Phys. Rev. D*, 102(7):072004.

[Aprile et al., 2022] Aprile, E. et al. (2022). Search for New Physics in Electronic Recoil Data from XENONnT. *Phys. Rev. Lett.*, 129(16):161805.

[Binetruy et al., 1984] Binetruy, P., Girardi, G., and Salati, P. (1984). Constraints on a System of Two Neutral Fermions From Cosmology. *Nucl. Phys. B*, 237:285–306.

[Blas et al., 2011] Blas, D., Lesgourgues, J., and Tram, T. (2011). The Cosmic Linear Anisotropy Solving System (CLASS) II: Approximation schemes. *JCAP*, 07:034.

[Boyarsky et al., 2009] Boyarsky, A., Ruchayskiy, O., and Iakubovskyi, D. (2009). A Lower bound on the mass of Dark Matter particles. *JCAP*, 03:005.

[Bullock and Boylan-Kolchin, 2017] Bullock, J. S. and Boylan-Kolchin, M. (2017). Small-Scale Challenges to the ΛCDM Paradigm. *Ann. Rev. Astron. Astrophys.*, 55:343–387.

[Carr et al., 2021] Carr, B., Kohri, K., Sendouda, Y., and Yokoyama, J. (2021). Constraints on primordial black holes. *Rept. Prog. Phys.*, 84(11):116902.

[Carr and Hawking, 1974] Carr, B. J. and Hawking, S. W. (1974). Black holes in the early Universe. *Mon. Not. Roy. Astron. Soc.*, 168:399–415.

[Corbelli and Salucci, 2000] Corbelli, E. and Salucci, P. (2000). The Extended Rotation Curve and the Dark Matter Halo of M33. *Mon. Not. Roy. Astron. Soc.*, 311:441–447.

[Dekker et al., 2022] Dekker, A., Ando, S., Correa, C. A., and Ng, K. C. Y. (2022). Warm dark matter constraints using Milky Way satellite observations and subhalo evolution modeling. *Phys. Rev. D*, 106(12):123026.

[Dine et al., 1981] Dine, M., Fischler, W., and Srednicki, M. (1981). A Simple Solution to the Strong CP Problem with a Harmless Axion. *Phys. Lett. B*, 104:199–202.

[Dodelson and Widrow, 1994] Dodelson, S. and Widrow, L. M. (1994). Sterile-neutrinos as dark matter. *Phys. Rev. Lett.*, 72:17–20.

[Famaey and McGaugh, 2012] Famaey, B. and McGaugh, S. (2012). Modified Newtonian Dynamics (MOND): Observational Phenomenology and Relativistic Extensions. *Living Rev. Rel.*, 15:10.

[Gervais and Sakita, 1971] Gervais, J.-L. and Sakita, B. (1971). Field Theory Interpretation of Supergauges in Dual Models. *Nucl. Phys. B*, 34:632–639.

[Hawking, 1971] Hawking, S. (1971). Gravitationally collapsed objects of very low mass. *Mon. Not. Roy. Astron. Soc.*, 152:75.

[Jedamzik, 1997] Jedamzik, K. (1997). Primordial black hole formation during the QCD epoch. *Phys. Rev. D*, 55:5871–5875.

[Kaluza, 1921] Kaluza, T. (1921). Zum unitätsproblem der physik. *Sitzungsber. Preuss. Akad. Wiss. Berlin (Math. Phys.)*, 1921(arXiv: 1803.08616):966–972.

[Kim, 1979] Kim, J. E. (1979). Weak Interaction Singlet and Strong CP Invariance. *Phys. Rev. Lett.*, 43:103.

[Klein, 1926] Klein, O. (1926). Quantum Theory and Five-Dimensional Theory of Relativity. (In German and English). *Z. Phys.*, 37:895–906.

[Leane et al., 2018] Leane, R. K., Slatyer, T. R., Beacom, J. F., and Ng, K. C. Y. (2018). GeV-scale thermal WIMPs: Not even slightly ruled out. *Phys. Rev. D*, 98(2):023016.

[Lee and Weinberg, 1977] Lee, B. W. and Weinberg, S. (1977). Cosmological Lower Bound on Heavy Neutrino Masses. *Phys. Rev. Lett.*, 39:165–168.

[Lesgourgues and Pastor, 2006] Lesgourgues, J. and Pastor, S. (2006). Massive neutrinos and cosmology. *Phys. Rept.*, 429:307–379.

[Lopez-Honorez et al., 2012] Lopez-Honorez, L., Schwetz, T., and Zupan, J. (2012). Higgs portal, fermionic dark matter, and a Standard Model like Higgs at 125 GeV. *Phys. Lett. B*, 716:179–185.

[Marsh, 2016] Marsh, D. J. E. (2016). Axion Cosmology. *Phys. Rept.*, 643:1–79.

[Milgrom, 1983] Milgrom, M. (1983). A Modification of the Newtonian dynamics as a possible alternative to the hidden mass hypothesis. *Astrophys. J.*, 270:365–370.

[Neveu and Schwarz, 1971] Neveu, A. and Schwarz, J. H. (1971). Factorizable dual model of pions. *Nucl. Phys. B*, 31:86–112.

[O'Hare, 2020] O'Hare, C. (2020). cajohare/axionlimits: Axionlimits. https://cajohare.github.io/AxionLimits/.

[Peccei and Quinn, 1977] Peccei, R. D. and Quinn, H. R. (1977). CP Conservation in the Presence of Instantons. *Phys. Rev. Lett.*, 38:1440–1443.

[Ramond, 1971] Ramond, P. (1971). Dual Theory for Free Fermions. *Phys. Rev. D*, 3:2415–2418.

[Shi and Fuller, 1999] Shi, X.-D. and Fuller, G. M. (1999). A New dark matter candidate: Nonthermal sterile neutrinos. *Phys. Rev. Lett.*, 82:2832–2835.

[Shifman et al., 1980] Shifman, M. A., Vainshtein, A. I., and Zakharov, V. I. (1980). Can Confinement Ensure Natural CP Invariance of Strong Interactions? *Nucl. Phys. B*, 166:493–506.

[Tremaine and Gunn, 1979] Tremaine, S. and Gunn, J. E. (1979). Dynamical Role of Light Neutral Leptons in Cosmology. *Phys. Rev. Lett.*, 42:407–410.

[Weinberg, 1978] Weinberg, S. (1978). A New Light Boson? *Phys. Rev. Lett.*, 40:223–226.

[Wess and Zumino, 1974] Wess, J. and Zumino, B. (1974). Supergauge Transformations in Four-Dimensions. *Nucl. Phys. B*, 70:39–50.

[Wilczek, 1978] Wilczek, F. (1978). Problem of Strong P and T Invariance in the Presence of Instantons. *Phys. Rev. Lett.*, 40:279–282.

[Zel'Dovich and Novikov, 1966] Zel'Dovich, Y. B. and Novikov, I. (1966). The hypothesis of cores retarded during expansion and the hot cosmological model. *Astronomicheskii Zhurnal*, 43:758.

[Zhitnitskij, 1980] Zhitnitskij, A. (1980). On possible suppression of the axion-hadron interactions. *Yadernaya Fizika*, 31(2):497–504.